# The quantum heat engine and heat pump: An irreversible thermodynamic analysis of the three-level amplifier

Eitan Geva[a] and Ronnie Kosloff
*Department of Physical Chemistry and the Fritz Haber Research Center, The Hebrew University, Jerusalem 91904, Israel*

(Received 22 December 1995; accepted 13 February 1996 )

The manifestations of the three laws of thermodynamics are explored in a model of an irreversible quantum heat engine. The engine is composed of a three-level system simultaneously coupled to hot and cold heat baths, and driven by an oscillating external field. General *quantum* heat baths are considered, which are weakly coupled to the three-level system. The work reservoir is modeled by a *classical* electro-magnetic field of arbitrary intensity, which is driving the three-level system. The first law of thermodynamics is related to the rate of change of energy obtained from the quantum master equation in the Heisenberg picture. The fluxes of the *thermodynamic* heat and work are then directly related to the expectation values of *quantum* observables. An analysis of the *standard* quantum master equation for the amplifier, first introduced by Lamb, is shown to be thermodynamically inconsistent when strong driving fields are used. A *generalized master equation* is rigorously derived, starting from the underlying quantum dynamics, which includes relaxation terms that explicitly depend upon the field. For weak fields the generalized master equation reduces to the standard equation. In *very intense* fields the amplifier splits into *two* heat engines. One engine accelerates as the field intensifies, while the other slows down and eventually switches direction to become a heat pump. The relative weight of the slower engine increases with the field intensity, leading to a maximum in power as a function of the field intensity. The amplifier is shown to go through four ''phases'' as the driving field is intensified, throughout all of which the second law of thermodynamics is generally satisfied. One phase corresponds to a ''refrigeration window'' which allows for the extraction of heat out of a cold bath of temperatures down to the absolute zero. This window disappears at absolute zero, which is conjectured to be a dynamical manifestation of the third law of thermodynamics.  [S0021-9606(96)50119-X]

## I. INTRODUCTION

The relationship between the theories of thermodynamics and quantum statistical mechanics is of fundamental importance. Numerous efforts have been devoted to establishing this relationship, and for three classes of systems it has been worked out:

- Systems at equilibrium (the Gibbs ensemble formalism[1]).
- Systems slightly distracted from equilibrium by the application of *small*, possibly time-dependent, external fields (linear response theory[2]).
- Systems *far* from equilibrium and coupled to heat baths that perform field-free relaxation towards an asymptotic equilibrium state (the quantum theory of open systems and the theory of quantum master equations[3,4]).

One class which is missing from this list consists of systems far from equilibrium, which are simultaneously coupled to heat baths and driven by *strong* external time-dependent fields. Many real heat engines and heat pumps, whose analysis by Carnot[5] marked the birth of thermodynamics, are based on such systems. In a modern context these systems are at the heart of spectroscopy and laser optics.[6,7] Statistical thermodynamics cannot be considered complete unless a full understanding of the thermodynamics of these systems is attained in terms of the underlying quantum dynamics.

Recently, a new road for studying irreversible thermodynamics has been established based on optimization of performance subject to *finite-rate constraints*. This approach, developed in the last two decades, has been denoted *Finite-Time Thermodynamics*.[8,9] The theory addresses such problems as the evaluation of the maximal work per cycle obtainable from a Carnot engine with a *finite* cycle duration.[10,11] The effect of other control parameters affecting irreversible performance was also considered. The results obtained differ from the reversible thermodynamical bounds which naturally correspond to infinitely slow processes.[12]

While also of practical interest, the dependence of the finite rate performance on various controls provides useful means for characterizing irreversibility. To this end the most appealing features of finite-time thermodynamics are:

- Thermodynamic processes are described in terms of *path* rather than *state* functions. Path functions are readily expressed in terms of quantum mechanical quantities regardless of the proximity to thermodynamic equilibrium.[3,13–15]
- It focuses upon the path integrated or steady-state

[a] Present address: Department of Chemistry, University of Wisconsin, Madison, Wisconsin 53706.

quantities directly affected by thermodynamic irreversibility.

Previous studies have utilized this approach to investigate irreversibility in quantum systems coupled to heat baths and driven by strong time-dependent external fields.[15–19] These studies established the framework for combining finite-time thermodynamics with quantum dynamics. Furthermore, the quantum statistical mechanical origin of some of the central results of finite-time thermodynamics was elucidated. Moreover the exclusive ways by which the irreversible thermodynamic performance is affected by the *quantum* nature of the underlying dynamics was studied for the first time.

The linkage between thermodynamics and quantum dynamics is obtained from a reduced description of the systems dynamics as given by the quantum master equation.[13] In the Heisenberg picture it becomes

$$\frac{d}{dt}\mathbf{X}=i[\mathbf{H_s^0}+\mathbf{W}(t),\mathbf{X}]+\frac{\partial}{\partial t}\mathbf{X}+\sum_i \mathscr{L}_D^i(\mathbf{X}). \tag{1.1}$$

Here, $\mathbf{X}$ is any system observable, $\mathbf{H_s^0}$ is the *stationary* free Hamiltonian of the system, $\mathbf{W}(t)$ is the interaction with the driving field, and $\mathscr{L}_D^i(\mathbf{X})$ is a dissipation term induced by the coupling to the $i$-th heat bath which is yet to be specified. (Throughout this paper, atomic units are used such that $\hbar=1$.)

The rate of energy change is obtained by substituting the full Hamiltonian of the system, $\mathbf{H}_s=\mathbf{H_s^0}+\mathbf{W}(t)$, for $\mathbf{X}$ in Eq. 1.1, leading to:

$$\frac{d}{dt}\mathbf{H_s}=\frac{\partial}{\partial t}\mathbf{W}+\sum_i \mathscr{L}_D^i(\mathbf{H_s}). \tag{1.2}$$

From a thermodynamic perspective, Eq. 1.2 is the time derivative of the first law of thermodynamics, identifying the heat flux from the $i$-th heat bath as

$$\dot{\mathscr{Q}}_i=\langle \mathscr{L}_D^i(\mathbf{H_s})\rangle, \tag{1.3}$$

and the work flux (power) as:[3,13–15]

$$\mathscr{P}=\langle \partial\mathbf{W}/\partial t\rangle. \tag{1.4}$$

The fundamental relations in Eqs. 1.3 and 1.4 provide the basis for the work presented in this paper.

The heat flux terms in Eq. 1.3 are derived for an open system driven by an external time-dependent field. Explicit expressions for these dissipative terms will be derived under the assumption that the interaction with the heat bath is much smaller than the energy of the free heat bath.[2,7,20,21] This assumption constitutes the quantum definition of a thermodynamic isothermal partition.[12] This implies that the heat bath remains in thermodynamic equilibrium, dissipating any fluctuation extremely fast on the time scale of the system's relaxation. This is frequently referred as the limit of motional narrowing.[7,22]

In analogy to the external pressure in the classical Carnot engine, the thermodynamic work reservoir is conceptually associated with an external driving field. From a quantum perspective, this requires a *semi-classical* treatment of the coupling with the driving field.[19,21,23] In this construction the alteration of the field by the system is ignored, while the system is influenced by the field, in accordance with the thermodynamic concept of the work reservoir.[12] However, the *time dependent* system-field interaction term must now be included in the system's Hamiltonian. Hence, the quantum master equation for a system with a non-stationary free Hamiltonian has to be derived. Such a quantum master equation generally involves heat flux terms which explicitly depend upon the field. This is in contrast to the assumption of weak coupling to the driving field, which renders those *relaxation* terms field independent.[19,21,23] The standard Bloch equations is a generic example of the weak coupling approach.[22–24] This approach is second order in the field and in the coupling to the bath. It is therefore able to account for the non-linear saturation at higher fields.[14] However, from the points of view of both theory and spectroscopic empiricism, the assumption of second order weak coupling to the field fails when it comes to higher fields,[19,25–46] where some of the most interesting thermodynamics hides.

Going beyond the limit of weak coupling to the field is crucial for a thermodynamic analysis. In general this leads to explicitly field-dependent relaxation terms. One limiting case, the ''slow field regime,'' is when the changes in the field are slow compared to the bath fluctuations. The quantum master equation can be derived in this limit, leading to a system directed towards thermal equilibrium corresponding to the *instantaneous* full Hamiltonian, $\mathbf{H_s}(t)$, unlike the time independent case which is directed toward equilibrium corresponding to the field-free Hamiltonian $\mathbf{H_s^0}$. The applicability condition of this approach depends on the type of the field driven Hamiltonian:[19,21]

- If the field-driven Hamiltonian *commutes* with itself at different times, $[\mathbf{H_s}(t),\mathbf{H_s}(t')]=0$, the variation of the field should be small on the time scale of the decay of bath fluctuations.
- If the field-driven Hamiltonian *does not commute* with itself at different times, $[\mathbf{H_s}(t),\mathbf{H_s}(t')]\neq 0$, then the variation of the field should be small over the time interval of the perturbation expansion with respect to the weak bath-system interaction (cf. Ref. 19).

Such a ''slow field'' approach has been applied in Refs. 16–18.

For the opposite and important case of *fast* driving fields, the quantum master equation can be derived if the field rotates at a constant frequency. This was demonstrated by Bloch and Tomita who, within the context of magnetic resonance, generalized the standard Bloch equations to strong rotating fields.[27,28] In a recent paper these equations have been re-derived within a more general context[19] and shown to be thermodynamically consistent for a driving field of arbitrary intensity. In contrast, the standard Bloch equation fails to do so at high fields, where they allow the complete conversion of heat into work, forbidden by the second law of thermodynamics.

The present study is devoted to the fundamental model of a quantum heat engine based on a three-level amplifier. The thermodynamical analogy has been pointed out by Geu-

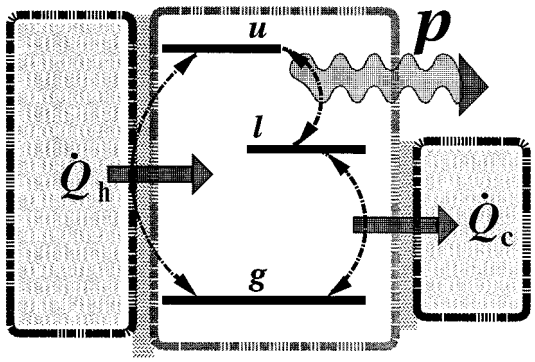


FIG. 1. A schematic view of the quantum three-level amplifier. $\mathscr{P}$, $\dot{Q}_h$ and $\dot{Q}_c$ are the steady-state power and fluxes of heat exchange with the hot and cold baths, respectively.

sic, Scovil and Schultz du Bois,[47–49] and later by Levine and Kafri[50] and Levine and Ben Shaul.[51] Following their argument, consider an array of non-interacting three-level atoms, each with energy levels as in Fig. 1. The setup is such that the transition between the lower and upper level is constantly excited (*pumped*), while the transition between the intermediate and lower level is constantly de-excited (*cooled*). Finally, the transition between the intermediate and upper levels is coupled to a monochromatic radiation that is driving the atoms. Efficient pumping and cooling would induce lasting *population inversion* between the two upper levels, thereby leading to *stimulated emission*. The stimulated emission is coherent with the driving field and hence constructively add to it, thereby leading to amplification.

Combining many such amplifiers with a cavity leads to laser action. In a laser the radiation is locked inside the cavity and gradually builds up by the amplification process. Describing this process would require coupling the dynamics of the system to that of the field build-up, i.e. the simultaneous solution of the Maxwell and Liouville equations.[7] This, however, would be in conflict with the thermodynamic concept of an infinite work reservoir. To avoid this complication it is assumed that the three-level atoms are arranged in a thin layer and illuminated by a radiation field of constant intensity. In this construction the amplified field is carried away by the outgoing light rays.

The qualitative analogy of this light amplification scheme to the action of a heat engine is obtained by associating the pumping with a coupling to a hot bath, the cooling with a coupling to a cold bath, and the electro-magnetic driving field with the work reservoir. In steady-state the energy of the array of three-level atoms remains fixed. Hence, all the heat absorbed from the hot bath is completely released as heat rejected into the cold bath and work added to the driving field, as in the generic heat engine. The flux balance is a statement of Kirchhoff's law, representing the first law of thermodynamics.

The examination of the second law of thermodynamics is more subtle. First the case of *weak* driving fields is considered. Transitions induced by the weak field hardly perturb the equilibrium Boltzmann distribution such that the ratio of occupancies of the upper and intermediate levels is given by:

$$P_u/P_l \approx \exp[-\beta_h(E_u-E_g)]/\exp[-\beta_c(E_l-E_g)]. \quad (1.5)$$

$P_i$ represents the occupancy of the i-th level, and $\beta_h$ and $\beta_c$ are the inverse temperatures of the hot and cold baths, temperatures being measured in units of energy (cf. Fig. 1). The efficiency of the engine is determined by the ratio of the energy emitted as work to the energy absorbed from the hot bath:

$$\eta=(E_u-E_l)/(E_u-E_g). \quad (1.6)$$

The condition for population inversion, $P_u \geqslant P_l$, then turns out to be equivalent to the Carnot inequality: $\eta \leqslant 1-T_c/T_h$. Thus, the Carnot efficiency sets the upper limit to the efficiency of this engine. Operating the amplifier at the maximum Carnot efficiency requires infinitesimally small population inversion, corresponding to an infinitely slow, i.e. *reversible*, mode of operation. This observation is the manifestation of the universal character of the Carnot engine which sets the reversible limit for the operation of even this quantum engine.

The above considerations cannot provide a *quantitative* picture of the irreversible performance of the quantum heat engine. Complete thermal equilibrium with the two baths would imply zero heat fluxes which is only true at the reversible limit. The role of the driving field is then twofold: it must induce stimulated emission at the lasing transition, and at the same time perturb the thermal equilibria at the other transitions, thereby inducing finite rate of heat transfer (energy balance dictates that the rates of heat transfer and stimulated emission cancel each other in steady-state).

In order to obtain a *quantitative* picture of the irreversible performance of the quantum heat engine, the underlying dissipative dynamics has to be taken into account. This dynamics is described by a *quantum master equation*. The quantum master equations for the three-level amplifier in the limit of weak coupling to the field are known as the *Lamb* equations.[7,52] These Lamb equations are the three-level analogue of the two-level Bloch equations. For comparison, the standard Lamb equations are presented in Appendix A, where their violation of first principle physical properties at high fields are pointed out (see also Refs. 15 and 18). A finite-time thermodynamic analysis of a similar engine model had already been published in Ref. 18 in the *slow field* regime. The present study is dedicated to the opposite regime of a *rapidly* rotating CW driving field, which exhibits different thermodynamic features at high fields. The *generalized Lamb equations* are derived, analogous to the generalized Bloch equations of Ref. 19. The manifestations of the laws of thermodynamics embedded in these equations are explored with an emphasis on the behavior at high fields. It will also be shown that the semi-group equations *suggested* in the past by Kosloff for the very similar model of the parametric amplifier[15] are consistent with a special case of the generalized Lamb equations derived in this paper.

The plan of this paper is as follows: The basic model is described in Sec. II. The derivation of the *generalized quantum master equation* is outlined in Sec. III. The generalized

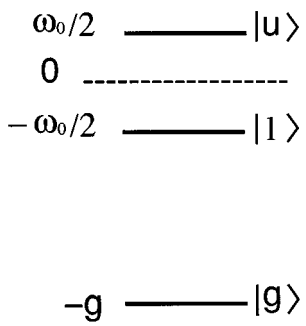


FIG. 2. The energy levels of the free three-level atoms constituting the working medium.

Lamb equations are then obtained in two convenient representations in Sec. IV. The latter are shown to coincide with the standard Lamb equations out of resonance or at the limit of weak fields in Sec. V. The deviations relative to the standard Lamb equations and their thermodynamic implications are then examined at moderately intense and very intense driving fields in Secs. VI and VII, respectively. An interpretation of the observations in terms of dressed states is also suggested, and the relationship with the semi-group generalized quantum master equation previously proposed by Kosloff for the parametric amplifier is indicated. The modes of operation scanned through as the driving field intensifies are described in Sec. VIII, and a ''refrigeration window'' which remains open down to a cold bath temperature of an absolute zero is shown to exist at high fields. The general results are demonstrated for the case of white baths in Sec. IX. Finally, the main results are summarized and possible extensions discussed in Sec. X.

## II. THE MODEL

The model is composed of an array of non-interacting three-level atoms. The energy level convention of each *free* three-level atom is shown in Fig 2. The zero in energy was chosen to lie in between the upper two levels for convenience. The Hamiltonian of the *extended* system, consisting of the three-level atom coupled to the field and the two heat baths, is given by:

$$\mathbf{H}=\mathbf{H_s^0}+\mathbf{W}(t)+\mathbf{H_h}+\mathbf{H_c}+\mathbf{H_{sh}}+\mathbf{H_{sc}}, \tag{2.1}$$

where $\mathbf{H_s^0}$ is the Hamiltonian of the free three-level atom, $\mathbf{W}(t)$ is the coupling term of the upper two levels to a *rotating* driving field, $\mathbf{H_h}$ and $\mathbf{H_c}$ are the free Hamiltonians of the hot and cold baths, and $\mathbf{H_{sh}}$, $\mathbf{H_{sc}}$ are the coupling terms of the three-level atom with the hot and cold baths:

$$\mathbf{H_s^0}=-g\mathbf{P_g}+\omega_0\mathbf{P_z}, \quad \mathbf{W}(t)=\epsilon(\mathbf{P}_+e^{-i\omega t}+\mathbf{P}_-e^{i\omega t}),$$
$$\mathbf{H_{sh}}=\delta\{\Lambda_h\otimes\mathbf{P_{u,g}}+\Lambda_h^\dagger\otimes\mathbf{P_{g,u}}+\Delta_h\otimes\tfrac{1}{2}(\mathbf{P_u}-\mathbf{P_g})\}, \tag{2.2}$$
$$\mathbf{H_{sc}}=\delta\{\Lambda_c\otimes\mathbf{P_{l,g}}+\Lambda_c^\dagger\otimes\mathbf{P_{g,l}}+\Delta_c\otimes\tfrac{1}{2}(\mathbf{P_l}-\mathbf{P_g})\}.$$

Here, $\mathbf{P_{i,j}}=|i\rangle\langle j|$, $\mathbf{P_i}=\mathbf{P_{i,i}}$, $\mathbf{P_z}=\frac{1}{2}(\mathbf{P_u}-\mathbf{P_l})$, $\mathbf{P}_+=\mathbf{P_{u,l}}$, $\mathbf{P}_-=\mathbf{P_{l,u}}$. $\Lambda_i$, $\Lambda_i^\dagger$ and $\Delta_i$ are operators of the i-th bath such that, with no loss of generality, $\langle\Lambda_i\rangle=0$, $\langle\Lambda_i^\dagger\rangle=0$ and $\langle\Delta_i\rangle=0$ at thermal equilibrium.[19] $\delta$ is the coupling constant to the baths on which the perturbation expansion is based. An important assumption is that the two heat baths consist of different and independent quantum systems.

## III. OUTLINE OF THE DERIVATION OF THE GENERALIZED QUANTUM MASTER EQUATION

The generalized quantum master equations for the three-level amplifier are derived by extending the method used previously in Ref. 19. In that study the generalized Bloch equations were derived for a two-level system coupled to a single heat bath and driven by a strong field. Hence, only an outline of the derivation is given, with emphasis on the differences between the two cases.

The first step is a transformation to the interaction picture. The latter is based on the partition of the total Hamiltonian, Eq. 2.1, into a zero Hamiltonian, $\mathbf{H_0}$, and a perturbation term, $\mathbf{H}'$, such that $\mathbf{H_0}=\mathbf{H_s^0}+\mathbf{W}(t)+\mathbf{H_h}+\mathbf{H_c}$ and $\mathbf{H}'=\mathbf{H_{sh}}+\mathbf{H_{sc}}$. The inclusion of the interaction with the field in the zero Hamiltonian means that it is treated exactly to all orders. It also means that the dynamics induced by $\mathbf{H_0}$ are solved in closed form in the case of a rotating field. The transformation to the interaction picture is in this case equivalent to the following two subsequent sub-steps: a transformation to the rotating frame, followed by a transformation to the interaction picture with respect to the stationary effective zero Hamiltonian in the rotating frame. The rest of the derivation is carried out in the rotating frame. For convenience the equations are derived in the eigenrepresentation of the effective Hamiltonian in the rotating frame, denoted the $\Pi$ representation, and then finally transformed to the original eigen representation of $\mathbf{H_s^0}$, denoted the $P$ representation.

Following the transformation to the interaction picture, $\mathbf{H}'$ is obtained in the $\Pi$ representation as a sum of *eight* independent terms. For comparison, the analogous expression in the case of the two-level system only contains three independent terms (Eq. (4.7) in Ref. 19). Each of these eight terms is a tensor product of a three-level atom operator and a bath operator. Each of the latter is a sum of *one* hot bath operator and *one* cold bath operator, with field-dependent coefficients. Only three combinations of bath operators occur in these terms, namely: $\Lambda_h$ with $\Lambda_c$, $\Lambda_h^\dagger$ with $\Lambda_c^\dagger$, and $\Delta_h$ with $\Delta_c$. Proceeding as in Ref. 19, the equation of motion for the reduced density operator of the three-level atom is obtained after truncating the perturbation expansion at second order in $\delta$ and taking a partial trace over the baths. The density operator maintains the form of a *single* tensor product, $\sigma\otimes\rho_h\otimes\rho_c$, throughout the entire evolution. Here $\sigma$ is the reduced density operator of the three-level atom, and $\rho_i=\exp(-\beta_i\mathbf{H_i})/\mathrm{Tr}_i[\exp(-\beta_i\mathbf{H_i})]$ is the thermal equilibrium density operator of the i-th bath ($i=c$ or $h$). The generalized quantum master equation for the amplifier contains $8^2=64$ terms in comparison to the $3^2=9$ terms in the analogous equation for the two-level system (Eq. (4.24) in Ref. 19).

A straightforward evaluation of these 64 terms, each leading to $2^2=4$ bath correlation functions, is extremely te-

dious. To reduce the effective number of terms to a tractable minimum the following properties were employed:

- Using the property that the two baths are independent the terms involving products of $\Lambda_h$, $\Lambda_h^\dagger$ or $\Delta_h$ (generally denoted by $\Gamma_h$) with $\Lambda_c$, $\Lambda_c^\dagger$ or $\Delta_c$ (generally denoted by $\Gamma_c$) do not contribute:

$$\mathrm{Tr}_b\{[\Gamma_c(t)\otimes\Gamma_h(t')][\rho_h\otimes\rho_c]\}=\langle\Gamma_c\rangle_c\times\langle\Gamma_h\rangle_c=0. \tag{3.1}$$

  Here $\mathrm{Tr}_b(\cdots)=\mathrm{Tr}_h\mathrm{Tr}_c(\cdots)$ correspond to partial traces over the Hilbert spaces of the hot and cold baths, and $\Gamma_j(\tau)=\exp(i\mathbf{H_j}\tau)\Gamma_j\exp(-i\mathbf{H_j}\tau)$.
- Terms rotating like $\exp(\pm i\omega t)$ and $\exp(\pm i\omega t/2)$ average out in the high-frequency regime.[19] Hence, terms involving products of $\Lambda_h$ or $\Lambda_c$ with $\Lambda_h$ or $\Lambda_c$, $\Lambda_h^\dagger$ or $\Lambda_c^\dagger$ with $\Lambda_h^\dagger$ or $\Lambda_c^\dagger$, $\Lambda_h$ or $\Lambda_c$ with $\Delta_h$ or $\Delta_c$, and $\Lambda_h^\dagger$ or $\Lambda_c^\dagger$ with $\Delta_h$ or $\Delta_c$ fall out.
- Among the 24 remaining terms ten pairs of hermitian conjugates are identified by using the following identity:

$$\{\mathrm{Tr}_b([\mathbf{A}\otimes\alpha,[\mathbf{B}\otimes\beta,\rho_b\otimes\sigma]])\}^\dagger = \mathrm{Tr}_b([\mathbf{A}^\dagger\otimes\alpha^\dagger,[\mathbf{B}^\dagger\otimes\beta^\dagger,\rho_b\otimes\sigma]]). \tag{3.2}$$

The effective number of terms is reduced to fourteen by use of the above properties. The bath factors in each of these fourteen terms are then evaluated by coarse-graining, i.e. by assuming that the bath correlations decay very fast on the time scale of the system's relaxation. Since the primary interest is in the relaxation dynamics, the imaginary parts of the bath factors, which are of the Lamb shift type, are neglected. The resulting bath factors consist of linear combinations of the Fourier transforms of bath correlation functions. The latter are listed in Table I, where

$$\widetilde{C}^j_{\Gamma\Gamma'}(x)=\int_{-\infty}^{\infty}d\tau e^{ix\tau}C^j_{\Gamma\Gamma'}(\tau), \tag{3.3}$$

$$C^j_{\Gamma\Gamma'}(\tau)=\mathrm{Tr}_j[\rho_i e^{i\mathbf{H}_j t}\Gamma e^{-i\mathbf{H}_j t}\Gamma'], \tag{3.4}$$

$$\Delta\omega=\omega_0-\omega, \tag{3.5}$$

$$\nu=\sqrt{(\Delta\omega)^2+(2\epsilon)^2}. \tag{3.6}$$

$\Delta\omega$ is the detuning and $\nu$ is the generalized Rabi frequency which reduces to the standard Rabi frequency, $2\epsilon$, at resonance, $\Delta\omega=0$. The resulting generalized quantum master equation was then transformed to the Heisenberg picture (cf. Appendix C in Ref. 19). The general form of this Heisenberg generalized quantum master equation is presented in detail in Appendix B, where it is also shown to provide justification and generalization to the quantum master equation proposed by Kosloff in Ref. 15.

TABLE I. The baths' parameters.

| | | | |
|---|---|---|---|
| $\lambda_h^{\pm}$ | $\widetilde{C}^h_{\Lambda\Lambda^\dagger}(g+\omega/2\pm\nu/2)$ | $\overline{\lambda_h^{\pm}}$ | $e^{-\beta_h(g+\omega/2\pm\nu/2)}\widetilde{C}^h_{\Lambda\Lambda^\dagger}(g+\omega/2\pm\nu/2)$ |
| $\lambda_c^{\pm}$ | $\widetilde{C}^c_{\Lambda\Lambda^\dagger}(g-\omega/2\pm\nu/2)$ | $\overline{\lambda_c^{\pm}}$ | $e^{-\beta_c(g-\omega/2\pm\nu/2)}\widetilde{C}^c_{\Lambda\Lambda^\dagger}(g-\omega/2\pm\nu/2)$ |
| $\delta_h^1$ | $\widetilde{C}^h_{\Delta\Delta}(\nu)$ | $\overline{\delta_h^1}$ | $e^{-\beta_h\nu}\widetilde{C}^h_{\Delta\Delta}(\nu)$ |
| $\delta_c^1$ | $\widetilde{C}^c_{\Delta\Delta}(\nu)$ | $\overline{\delta_c^1}$ | $e^{-\beta_c\nu}\widetilde{C}^c_{\Delta\Delta}(\nu)$ |
| $\delta_h^0$ | $\widetilde{C}^h_{\Delta\Delta}(0)$ | $\delta_c^0$ | $\widetilde{C}^c_{\Delta\Delta}(0)$ |

## IV. THE GENERALIZED LAMB EQUATIONS

The state of a three-level atom is fully characterized by the expectation values of any *eight* independent operators, excluding the identity operator. Each choice of eight independent operators corresponds to a different representation. The following two representations were found convenient, in analogy to the corresponding representations used for the two-level system in Ref. 19 (cf. Eqs. (4.29) and (4.34) there):

- *The P representation*, which is the eigenrepresentation of the *free* Hamiltonian, $\mathbf{H_s^0}$, in the rotating frame:

$$\hat{\mathbf{P}}_{\mathbf{i,j}}=e^{-i\omega\mathbf{P}_z t}\mathbf{P}_{\mathbf{i,j}}e^{i\omega\mathbf{P}_z t}. \tag{4.1}$$

The following notations are also used, in analogy to Ref. 19: $\hat{\mathbf{P}}_\mathbf{i}=\hat{\mathbf{P}}_{\mathbf{ii}}$, $\hat{\mathbf{P}}_+=\hat{\mathbf{P}}_{\mathbf{ul}}$, $\hat{\mathbf{P}}_-=\hat{\mathbf{P}}_{\mathbf{lu}}$, $\hat{\mathbf{P}}_\mathbf{x}=\frac{1}{2}(\hat{\mathbf{P}}_+ +\hat{\mathbf{P}}_-)$, $\hat{\mathbf{P}}_\mathbf{y}=\frac{1}{2i}(\hat{\mathbf{P}}_+ -\hat{\mathbf{P}}_-)$, $\hat{\mathbf{P}}_\mathbf{z}=\frac{1}{2}(\hat{\mathbf{P}}_\mathbf{u}-\hat{\mathbf{P}}_\mathbf{l})$. Note that the populations in this representation, $\{\mathbf{P_i}\}$, are invariant under the transformation to the rotating frame: $\hat{\mathbf{P}}_\mathbf{i}=\mathbf{P_i}$. Hence, $\hat{\mathbf{H}}_\mathbf{s}^\mathbf{0}=\mathbf{H}_\mathbf{s}^\mathbf{0}$.

- *The* $\Pi$ *representation*, which is the eigenrepresentation of the *full* Hamiltonian in the rotating frame, $\hat{\mathbf{H}}_\mathbf{s}=\hat{\mathbf{H}}_\mathbf{s}^\mathbf{0}+\hat{\mathbf{W}}$:

$$\hat{\mathbf{\Pi}}_{\mathbf{i,j}}=e^{-i\theta\hat{\mathbf{P}}_\mathbf{y}}\hat{\mathbf{P}}_{\mathbf{i,j}}e^{i\theta\hat{\mathbf{P}}_\mathbf{y}}, \tag{4.2}$$

  where $\tan(\theta)=2\epsilon/\Delta\omega$. Note that $\hat{\mathbf{H}}_\mathbf{s}^\mathbf{0}+\hat{\mathbf{W}}=\Delta\omega\hat{\mathbf{P}}_\mathbf{z}+2\epsilon\hat{\mathbf{P}}_\mathbf{x}=\nu\mathbf{\Pi}_\mathbf{z}$. Further notation is introduced by $\hat{\mathbf{\Pi}}_\mathbf{i},\hat{\mathbf{\Pi}}_\pm$, $\hat{\mathbf{\Pi}}_\mathbf{x},\hat{\mathbf{\Pi}}_\mathbf{y},\hat{\mathbf{\Pi}}_\mathbf{z}$, defined in a similar manner to the analogous operators in the *P* representation, provided that each $\mathbf{P}$ is replaced by a $\mathbf{\Pi}$. The $\Pi$ representation coincides with the atom-field dressed state representation.[53]

The standard Lamb equations are given in terms of four observables: $\hat{\mathbf{P}}_+$, $\hat{\mathbf{P}}_-$, $\hat{\mathbf{P}}_\mathbf{u}$, $\hat{\mathbf{P}}_\mathbf{l}$ (cf. Eq. A1). This is possible since the power and heat fluxes depend only on this subset, which is decoupled from the rest of the operators. Fortunately, this property is retained by the generalized quantum master equation, which can be given in terms of one of the two subsets: $\{\hat{\mathbf{P}}_+,\hat{\mathbf{P}}_-,\hat{\mathbf{P}}_\mathbf{u},\hat{\mathbf{P}}_\mathbf{l}\}$ or $\{\hat{\mathbf{\Pi}}_+,\hat{\mathbf{\Pi}}_-,\hat{\mathbf{\Pi}}_\mathbf{u},\hat{\mathbf{\Pi}}_\mathbf{l}\}$. It is possible to obtain the generalized quantum master equation for the rest of the operators, say $\hat{\mathbf{P}}_{g,l},\hat{\mathbf{P}}_{l,g},\hat{\mathbf{P}}_{g,u}$ and $\hat{\mathbf{P}}_{u,g}$ in the *P* representation, and to show that they vanish in steady-state.

Finally, the relaxation coefficients in the generalized Lamb equations are given in terms of the field-dependent bath parameters listed in Table I. If $\omega\pm\nu$ and $\nu$ are substituted by $\omega_0$ and 0, respectively, the following correspondence with the *standard* rate coefficients is established (cf. Eq. A2): $\lambda_i^{\pm}\rightarrow\lambda_i^0$; $\overline{\lambda_i^{\pm}}\rightarrow\overline{\lambda_i^0}$; $\delta_i^1,\overline{\delta_i^1}\rightarrow\delta_i^0$.

### A. The generalized Lamb equations in the *P* representation

Choosing the conventional *P* representation, the generalized Lamb equations become:

$$\frac{d}{dt}\begin{pmatrix}\hat{\mathbf{P}}_+\\ \hat{\mathbf{P}}_-\\ \hat{\mathbf{P}}_\mathbf{u}\\ \hat{\mathbf{P}}_\mathbf{l}\end{pmatrix}=\begin{pmatrix} i\Delta\omega+\Gamma_+ & 0 & -i\epsilon+\Gamma_{+u} & i\epsilon+\Gamma_{+l}\\ 0 & -i\Delta\omega+\Gamma_- & i\epsilon+\Gamma_{-u} & -i\epsilon+\Gamma_{-l}\\ -i\epsilon+\Gamma_{u+} & i\epsilon+\Gamma_{u-} & \Gamma_u & \Gamma_{ul}\\ i\epsilon+\Gamma_{l+} & -i\epsilon+\Gamma_{l-} & \Gamma_{lu} & \Gamma_l\end{pmatrix}\begin{pmatrix}\hat{\mathbf{P}}_+\\ \hat{\mathbf{P}}_-\\ \hat{\mathbf{P}}_\mathbf{u}\\ \hat{\mathbf{P}}_\mathbf{l}\end{pmatrix}+\begin{pmatrix}\gamma_+\\ \gamma_-\\ \gamma_u\\ \gamma_l\end{pmatrix}. \tag{4.3}$$

The relaxation coefficients $\{\Gamma_{i,j},\Gamma_i,\gamma_i\}$ consist of linear combinations of the bath parameters of Table I. The coefficients of the off-diagonal coupling parameters $(\lambda_c^{\pm},\lambda_h^{\pm},\overline{\lambda_c^{\pm}},\overline{\lambda_h^{\pm}})$ and the diagonal coupling parameters $(\delta_c^{0/1},\delta_h^{0/1},\overline{\delta_c^{0/1}},\overline{\delta_h^{0/1}})$ are explicitly given in Tables II and III, respectively.

### B. The generalized Lamb equations in the Π representation

Choosing the Π representation, as suggested by Kosloff in Ref. 15, the generalized Lamb equations are cast into the following form:

$$\frac{d}{dt}\begin{pmatrix}\hat{\mathbf{\Pi}}_+\\ \hat{\mathbf{\Pi}}_-\\ \hat{\mathbf{\Pi}}_\mathbf{u}\\ \hat{\mathbf{\Pi}}_\mathbf{l}\end{pmatrix}=\begin{pmatrix} i\nu+\Phi_+ & \Phi_{+-} & \Phi_{+u} & \Phi_{+l}\\ \Phi_{-+} & -i\nu+\Phi_- & \Phi_{-u} & \Phi_{-l}\\ \Phi_{u+} & \Phi_{u-} & \Phi_u & \Phi_{ul}\\ \Phi_{l+} & \Phi_{l-} & \Phi_{lu} & \Phi_l\end{pmatrix}\times\begin{pmatrix}\hat{\mathbf{\Pi}}_+\\ \hat{\mathbf{\Pi}}_-\\ \hat{\mathbf{\Pi}}_\mathbf{u}\\ \hat{\mathbf{\Pi}}_\mathbf{l}\end{pmatrix}+\begin{pmatrix}\phi_+\\ \phi_-\\ \phi_u\\ \phi_l\end{pmatrix}. \tag{4.4}$$

The relaxation coefficients $\{\Phi_{i,j},\Phi_i,\phi_i\}$ also consist of linear combinations of the bath parameters of Table I. The coefficients of the off-diagonal coupling parameters $(\lambda_c^{\pm},\lambda_h^{\pm},\overline{\lambda_c^{\pm}},\overline{\lambda_h^{\pm}})$ and the diagonal coupling parameters $(\delta_c^{0/1},\delta_h^{0/1},\overline{\delta_c^{0/1}},\overline{\delta_h^{0/1}})$ are explicitly given in Tables IV and V, respectively.

## V. THE DOMAIN OF WEAK DRIVING FIELDS

The standard Lamb equations are valid when the coupling of the three-level atoms to the driving field is of the same order of magnitude as the coupling with the heat baths, i.e. when $\epsilon\sim\lambda_i^{\pm},\overline{\lambda_i^{\pm}},\delta_i^1,\overline{\delta_i^1},\delta_i^0$. Indeed, the standard Lamb equations, Eq. A1, are retrieved from the generalized ones in the $P$ representation, Eq. 4.3, at one of two complementary limits:

- The limit where $|\Delta\omega|\gg|2\epsilon|$. In this case $\nu\to|\Delta\omega|$, $\sin(\theta)\to 0$ and $\cos(\theta)\to\pm 1$, depending on the sign of $\Delta\omega$. By substituting these asymptotic values into the generalized Lamb equations, Eq. 4.3, it coincides with the standard Lamb equations, Eq. A1. This behavior is expected since tuning the field out of resonance is equivalent to turning it off, and is often used this way in practice.

TABLE II. The contribution of off-diagonal couplings to the relaxation coefficients in the $P$ representation. $c$ and $s$ stand for $\cos\theta$ and $\sin\theta$, respectively, where $\tan\theta=2\epsilon/\Delta\omega$.

| | $\lambda_h^+$ | $\overline{\lambda_h^+}$ | $\lambda_h^-$ | $\overline{\lambda_h^-}$ | $\lambda_c^+$ | $\overline{\lambda_c^+}$ | $\lambda_c^-$ | $\overline{\lambda_c^-}$ |
|---|---|---|---|---|---|---|---|---|
| $\gamma_\pm$ | - | $\frac{s}{4}$ | - | $-\frac{s}{4}$ | - | $\frac{s}{4}$ | - | $-\frac{s}{4}$ |
| $\gamma_u$ | - | $\frac{1+c}{2}$ | - | $\frac{1-c}{2}$ | - | - | - | - |
| $\gamma_l$ | - | - | - | - | - | $\frac{1-c}{2}$ | - | $\frac{1+c}{2}$ |
| $\Gamma_\pm$ | $-\frac{1+c}{4}$ | - | $-\frac{1-c}{4}$ | - | $-\frac{1-c}{4}$ | - | $-\frac{1+c}{4}$ | - |
| $\Gamma_{\pm u}$ | - | $-\frac{s}{4}$ | - | $\frac{s}{4}$ | $-\frac{s}{4}$ | $-\frac{s}{4}$ | $\frac{s}{4}$ | $\frac{s}{4}$ |
| $\Gamma_{\pm l}$ | $-\frac{s}{4}$ | $-\frac{s}{4}$ | $\frac{s}{4}$ | $\frac{s}{4}$ | - | $-\frac{s}{4}$ | - | $\frac{s}{4}$ |
| $\Gamma_{u\pm}$ | $-\frac{s}{4}$ | - | $\frac{s}{4}$ | - | - | - | - | - |
| $\Gamma_{l\pm}$ | - | - | - | - | $-\frac{s}{4}$ | - | $\frac{s}{4}$ | - |
| $\Gamma_u$ | $-\frac{1+c}{2}$ | $-\frac{1+c}{2}$ | $-\frac{1-c}{2}$ | $-\frac{1-c}{2}$ | - | - | - | - |
| $\Gamma_l$ | - | - | - | - | $-\frac{1-c}{2}$ | $-\frac{1-c}{2}$ | $-\frac{1+c}{2}$ | $-\frac{1+c}{2}$ |
| $\Gamma_{ul}$ | - | $-\frac{1+c}{2}$ | - | $-\frac{1-c}{2}$ | - | - | - | - |
| $\Gamma_{lu}$ | - | - | - | - | - | $-\frac{1-c}{2}$ | - | $-\frac{1+c}{2}$ |

TABLE III. The contribution of diagonal couplings to the relaxation coefficients in the $P$ representation. $c$ and $s$ stand for $\cos\theta$ and $\sin\theta$, respectively, where $\tan\theta=2\epsilon/\Delta\omega$.

| | $\delta_h^0$ | $\delta_c^0$ | $\delta_h^1$ | $\overline{\delta_h^1}$ | $\delta_c^1$ | $\overline{\delta_c^1}$ |
|---|---|---|---|---|---|---|
| $\Gamma_{\pm}$ | $-\frac{c^2}{8}$ | $-\frac{c^2}{8}$ | $-\frac{s^2}{16}$ | $-\frac{s^2}{16}$ | $-\frac{s^2}{16}$ | $-\frac{s^2}{16}$ |
| $\Gamma_{\pm u}$ | $\frac{sc}{16}$ | $\frac{sc}{16}$ | $-\frac{s(1+c)}{32}$ | $\frac{s(1-c)}{32}$ | $-\frac{s(1+c)}{32}$ | $\frac{s(1-c)}{32}$ |
| $\Gamma_{\pm l}$ | $-\frac{sc}{16}$ | $-\frac{sc}{16}$ | $-\frac{s(1-c)}{32}$ | $\frac{s(1+c)}{32}$ | $-\frac{s(1-c)}{32}$ | $\frac{s(1+c)}{32}$ |

- The limit $|2\epsilon|,|\Delta\omega|\ll\omega_0,1/\tau_c^{\Delta}$, where $1/\tau_c^{\Delta}$ is the characteristic rate of decay of the *diagonal* bath correlation functions, $C^i_{\Delta\Delta}(\tau)$. In this case, $\nu\ll 1/\tau_c^{\Delta},\omega_0\approx\omega$ and hence $\lambda_i^{\pm}\to\lambda_i^0;\overline{\lambda_i^{\pm}}\to\overline{\lambda_i^0}$; $\delta_i^1,\overline{\delta_i^1}\to\delta_i^0$. Once again, these asymptotic values turn the generalized Lamb equations into the standard ones. Thus, the standard Lamb equations are also valid at resonance and its close vicinity, provided the coupling with the field is sufficiently weak.

Whereas the fact that the generalized Lamb equations converge to the standard ones at weak driving fields is not surprising, the discussion above provides a quantitative measure as to the meaning of a *weak driving field*. It also clarifies the point that as $\epsilon$ increases beyond $\Delta\omega$ or $1/\tau_c^{\Delta}$ and $\omega_0$, deviations are expected from the standard Lamb equations. These deviations are explored in the following sections.

## VI. THE DOMAIN OF MODERATELY INTENSE DRIVING FIELDS

For a driving field of moderate intensity: $1/\tau_c^{\Delta}\ll\nu\ll\omega_0$. The terms associated with the off-diagonal coupling to the baths become identical to the standard Lamb equations since in this case $\lambda_i^{\pm}\to\lambda_i^0$ and $\overline{\lambda_i^{\pm}}\to\overline{\lambda_i^0}$ (cf. Sec. V). However, since $e^{i\nu t}$ oscillates many times before $C^i_{\Delta\Delta}(\tau)$ can change appreciably, $\tilde{C}^i_{\Delta\Delta}(\nu)$ vanishes in this domain.[19] Thus, $\delta_i^1$ and $\overline{\delta_i^1}$ are negligible under such moderately intense fields.

Referring to Table III, the only relaxation coefficients which *differ* from the standard Lamb coefficients are $\Gamma_{\pm}$, $\Gamma_{\pm u}$ and $\Gamma_{\pm l}$. In the domain of moderate driving fields, and recalling that $\tan(\theta)=2\epsilon/\Delta\omega$, the latter are approximately given by:

$$\Gamma_{\pm}\approx-\frac{1}{2}(\lambda_h^0+\lambda_c^0)-\frac{1}{8}\frac{(\Delta\omega)^2}{(\Delta\omega)^2+(2\epsilon)^2}(\delta_h^0+\delta_c^0),$$
$$\Gamma_{\pm u}=-\Gamma_{\pm l}\approx\frac{1}{16}\frac{2\epsilon\Delta\omega}{(\Delta\omega)^2+(2\epsilon)^2}(\delta_h^0+\delta_c^0). \tag{6.1}$$

In the close vicinity of resonance, $|2\epsilon|\gg|\Delta\omega|$, one obtains $\Gamma_{\pm}\to-\frac{1}{2}(\lambda_h^0+\lambda_c^0)$ while $\Gamma_{\pm u},\Gamma_{\pm l}\to 0$. Thus, under a moderately intense driving field, the generalized Lamb equations coincide with the standard Lamb equations with the diagonal couplings suppressed. A similar quenching of the diagonal coupling, ''pure dephasing,'' terms was experimentally observed[31–33] and theoretically predicted[19,34–46] in the analogous treatment for a two-level system. It should be noted that

TABLE IV. The contribution of off-diagonal couplings to the relaxation coefficients in the $\Pi$ representation. $c$ and $s$ stand for $\cos\theta$ and $\sin\theta$, respectively, where $\tan\theta=2\epsilon/\Delta\omega$.

| | $\lambda_h^+$ | $\overline{\lambda_h^+}$ | $\lambda_h^-$ | $\overline{\lambda_h^-}$ | $\lambda_c^+$ | $\overline{\lambda_c^+}$ | $\lambda_c^-$ | $\overline{\lambda_c^-}$ |
|---|---|---|---|---|---|---|---|---|
| $\phi_{\pm}$ | - | $-\frac{s}{4}$ | - | $-\frac{s}{4}$ | - | $\frac{s}{4}$ | - | $\frac{s}{4}$ |
| $\phi_u$ | - | $\frac{1+c}{2}$ | - | - | - | $\frac{1-c}{2}$ | - | - |
| $\phi_l$ | - | - | - | $\frac{1-c}{2}$ | - | - | - | $\frac{1+c}{2}$ |
| $\Phi_{\pm}$ | $-\frac{1+c}{4}$ | - | $-\frac{1-c}{4}$ | - | $-\frac{1-c}{4}$ | - | $-\frac{1+c}{4}$ | - |
| $\Phi_{\pm u}$ | $\frac{s}{4}$ | $\frac{s}{4}$ | - | $\frac{s}{4}$ | $-\frac{s}{4}$ | $-\frac{s}{4}$ | - | $-\frac{s}{4}$ |
| $\Phi_{\pm l}$ | - | $\frac{s}{4}$ | $\frac{s}{4}$ | $\frac{s}{4}$ | - | $-\frac{s}{4}$ | $-\frac{s}{4}$ | $-\frac{s}{4}$ |
| $\Phi_{u\pm}$ | - | - | $\frac{s}{4}$ | - | - | - | $-\frac{s}{4}$ | - |
| $\Phi_{l\pm}$ | $\frac{s}{4}$ | - | - | - | $-\frac{s}{4}$ | - | - | - |
| $\Phi_u$ | $-\frac{1+c}{2}$ | $-\frac{1+c}{2}$ | - | - | $-\frac{1-c}{2}$ | $-\frac{1-c}{2}$ | - | - |
| $\Phi_l$ | - | - | $-\frac{1-c}{2}$ | $-\frac{1-c}{2}$ | - | - | $-\frac{1+c}{2}$ | $-\frac{1+c}{2}$ |
| $\Phi_{ul}$ | - | $-\frac{1+c}{2}$ | - | - | - | $-\frac{1-c}{2}$ | - | - |
| $\Phi_{lu}$ | - | - | - | $-\frac{1-c}{2}$ | - | - | - | $-\frac{1+c}{2}$ |

TABLE V. The contribution of diagonal couplings to the relaxation coefficients in the $\Pi$ representation. $c$ and $s$ stand for $\cos\theta$ and $\sin\theta$, respectively, where $\tan\theta=2\epsilon/\Delta\omega$.

| | $\delta_h^0$ | $\delta_c^0$ | $\delta_h^1$ | $\overline{\delta_h^1}$ | $\delta_c^1$ | $\overline{\delta_c^1}$ |
|---|---|---|---|---|---|---|
| $\Phi_{\pm}$ | $-\frac{c^2}{8}$ | $-\frac{c^2}{8}$ | $-\frac{s^2}{32}$ | $-\frac{s^2}{32}$ | $-\frac{s^2}{32}$ | $-\frac{s^2}{32}$ |
| $\Phi_{\pm\mp}$ | - | - | $\frac{s^2}{32}$ | $\frac{s^2}{32}$ | $\frac{s^2}{32}$ | $\frac{s^2}{32}$ |
| $\Phi_{\pm u}$ | - | - | $-\frac{sc}{16}$ | - | $-\frac{sc}{16}$ | - |
| $\Phi_{\pm l}$ | - | - | - | $\frac{sc}{16}$ | - | $\frac{sc}{16}$ |
| $\Phi_{u\pm}$ | $-\frac{sc}{16}$ | $-\frac{sc}{16}$ | - | - | - | - |
| $\Phi_{l\pm}$ | $\frac{sc}{16}$ | $\frac{sc}{16}$ | - | - | - | - |
| $\Phi_{u}$ | - | - | $-\frac{s^2}{16}$ | - | $-\frac{s^2}{16}$ | - |
| $\Phi_{l}$ | - | - | - | $-\frac{s^2}{16}$ | - | $-\frac{s^2}{16}$ |
| $\Phi_{ul}$ | - | - | - | $\frac{s^2}{16}$ | - | $\frac{s^2}{16}$ |
| $\Phi_{lu}$ | - | - | $\frac{s^2}{16}$ | - | $\frac{s^2}{16}$ | - |

the condition $|2\epsilon|\gg|\Delta\omega|$ is obtained by either decreasing $|\Delta\omega|$ or by increasing $|2\epsilon|$. Hence, at such intense fields, considerable deviation from resonance ($\Delta\omega=0$) occurs and still this condition is fulfilled. Summarizing, as the field intensifies, the line-shape broadens such that the amplified power becomes insensitive to the field frequency over a wide range.

## VII. THE DOMAIN OF VERY INTENSE DRIVING FIELDS

The domain of very intense fields is approached when the field amplitude $\epsilon$ becomes non-negligible relative to the frequency $\omega_0$ or even higher. At such intense driving fields, diagonal coupling with the baths is totally quenched out and ''resonance'' conditions, $|2\epsilon|\gg|\Delta\omega|$, prevail while still covering a very wide range of field frequencies (cf. Sec. VI). This considerably simplifies the description of the amplifier for intense fields. Unlike in the domain of moderately intense driving fields, the relaxation coefficients associated with off-diagonal coupling to the baths deviate relative to these in the standard Lamb equations. Substitution of $s=1$, $c=0$, and $\omega\pm\nu=\omega_0\pm\epsilon$ in the expressions of Tables II and IV considerably simplifies the relaxation coefficients at very intense fields. The physical picture behind the generalized Lamb equations obtained in this case is discussed in the following sub-sections.

### A. An interpretation of the $\Pi$ and *P* representations

The $\Pi$ representation is actually the eigen-representation of the *dressed Hamiltonian*.[53] The significance of this picture can be appreciated by considering *decoupling* the cold bath, i.e. putting $\lambda_c^{\pm}=0$. The three-level atoms will then relax to an *equilibrium* state where:

$$\hat{\Pi}_{\pm}^{eq,h}=0,\quad \hat{\Pi}_u^{eq,h}=\frac{n_h^+}{1+n_h^++n_h^-},\quad \hat{\Pi}_l^{eq,h}=\frac{n_h^-}{1+n_h^++n_h^-}, \tag{7.1}$$

and

$$n_h^{\pm}=\exp[-\beta_h(g+\omega_0/2\pm\epsilon)]. \tag{7.2}$$

This is an *equilibrium state* rather than *steady-state* since cyclic action is prohibited once the cold bath is decoupled. Thus, there is no energy exchange with the environment and no entropy production.

Decoupling the hot bath leads to a similar equilibrium state:

$$\hat{\Pi}_{\pm}^{eq,c}=0,\quad \hat{\Pi}_u^{eq,c}=\frac{n_c^+}{1+n_c^++n_c^-},\quad \hat{\Pi}_l^{eq,c}=\frac{n_c^-}{1+n_c^++n_c^-}, \tag{7.3}$$

where

$$n_c^{\pm}=\exp[-\beta_c(g-\omega_0/2\pm\epsilon)]. \tag{7.4}$$

From these considerations the $\hat{\Pi}_u$ and $\hat{\Pi}_l$ are interpreted as the populations of the dressed states shifted *upwards* and *downwards* in energy by $\epsilon$, respectively. These dressed states consist of superpositions of the original states. Hence, each of the dressed subspaces are relaxed by *both* baths. Furthermore, the relaxation terms satisfy detailed balance with respect to the manifold of dressed states, as is clearly seen from Eqs. 7.1 and 7.3. Kosloff previously proposed a simpler version of this structure in the case of the parametric amplifier, based on the requirement for detailed-balance in the dressed states manifold.[15] In the present work this structure has been *derived* from first principles and thereby rigorously justified and extended (cf. Appendix B for a more detailed discussion of the relationship to Ref. 15).

The above discussion invokes the following physical picture: Each of the heat baths is coupled with *two* three-level manifolds which correspond to the following sets of energy levels: $\{-g,-\omega_0/2+\epsilon,\omega_0/2+\epsilon\}$ and $\{-g,-\omega_0/2-\epsilon,\omega_0/2-\epsilon\}$. They are denoted below as the *upper manifold* and the *lower manifold*, respectively. The two excited states are shifted up or down in energy by $\epsilon$ relative to the free three-level atom. The expectation $\hat{\Pi}_u$ then corresponds to the total occupancy in the two levels of the upper manifold that got shifted up by $\epsilon$, whereas $\hat{\Pi}_l$ corresponds to the total occupancy in the two levels of the lower manifold that got shifted down by $\epsilon$. The populations in the *P* representation, on the other hand, correspond to different groupings of the energy levels. $P_l$ is the population of the level of energy $-\omega_0/2$ in the free atom, hence it corresponds to the total population in the two levels of energies $-\omega_0/2\pm\epsilon$ which it splits into when dressed by the field. Similarly, $P_u$ corre-

sponds to the total population in the two dressed levels of energies $\omega_0/2\pm\epsilon$. This situation is schematically described in Fig. 3.

### B. The steady-state power and heat flows at very intense fields

The most pronounced deviations from the standard Lamb equations occur in the domain of very intense fields. The thermodynamics implied by the generalized Lamb equations in the domain of very intense fields is analyzed. This is in contrast to the standard Lamb equations which are thermodynamically inconsistent in this domain (cf. Appendix A). The analysis is based on the steady-state power and heat flows which are evaluated by solving the generalized Lamb equations (Eq. 4.3 or 4.4). The evaluation is further simplified by the following conditions valid under intense fields:

- $\lambda_i^{\pm}$, $\overline{\lambda_i^{\pm}}$, $\lambda_i^{\pm}$ and $\overline{\lambda_i^{\pm}}$ are negligible relative to $\epsilon$.
- The diagonal coupling terms are completely suppressed (cf. Sec. VI).
- The ''resonance conditions'' are valid when $|\Delta\omega|\ll|2\epsilon|$. This assumption still allows for considerable deviations from resonance, $\Delta\omega=0$, due to power broadening.

The resulting steady-state power and heat flows are given by (cf. Eqs. 1.3 and 1.4):

$$\mathscr{P}^{ss}=-\frac{1}{Z}\omega_0[\lambda_h^+\lambda_c^+(\lambda_h^-+\lambda_c^-)(n_h^+-n_c^+)+\lambda_h^-\lambda_c^-(\lambda_h^+ +\lambda_c^+)(n_h^--n_c^-)], \tag{7.5}$$

$$\dot{\mathscr{Q}}_h^{ss}=\frac{1}{Z}\left[\left(g+\frac{\omega_0}{2}+\epsilon\right)\lambda_h^+\lambda_c^+(\lambda_h^-+\lambda_c^-)(n_h^+-n_c^+) +\left(g+\frac{\omega_0}{2}-\epsilon\right)\lambda_h^-\lambda_c^-(\lambda_h^++\lambda_c^+)(n_h^--n_c^-)\right], \tag{7.6}$$

$$\dot{\mathscr{Q}}_c^{ss}=-\frac{1}{Z}\left[\left(g-\frac{\omega_0}{2}+\epsilon\right)\lambda_h^+\lambda_c^+(\lambda_h^-+\lambda_c^-)(n_h^+-n_c^+) +\left(g-\frac{\omega_0}{2}-\epsilon\right)\lambda_h^-\lambda_c^-(\lambda_h^++\lambda_c^+)(n_h^--n_c^-)\right], \tag{7.7}$$

where

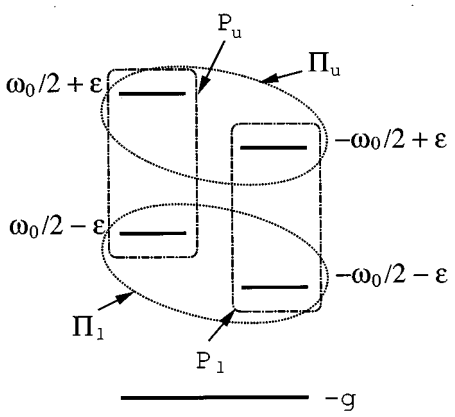


FIG. 3. The upper and lower manifolds and their interpretation in terms of the $P$ and $\Pi$ representations.

$$Z=2[(\lambda_h^++\lambda_c^+)(\lambda_h^-+\lambda_c^-)+(\overline{\lambda_h^+}+\overline{\lambda_c^+})(\lambda_h^-+\lambda_c^-) +(\lambda_h^++\lambda_c^+)(\overline{\lambda_h^-}+\overline{\lambda_c^-})]. \tag{7.8}$$

Eqs. 7.5–7.7 satisfy the first law of thermodynamics by obeying Kirchhoff's law $\dot{\mathscr{Q}}_h^{ss}+\dot{\mathscr{Q}}_c^{ss}+\mathscr{P}^{ss}=0$. It should be noted that the steady-state power and heat flows obtained from the standard Lamb equations also satisfy the first law of thermodynamics.

Turning next to the second law of thermodynamics, the steady-state rate of entropy production, $\dot{\Sigma}^{ss}$, is directly obtainable from Eqs. 7.5–7.7:

$$\begin{aligned}\dot{\Sigma}^{ss}&=-\dot{\mathscr{Q}}_h^{ss}/T_h-\dot{\mathscr{Q}}_c^{ss}/T_c\\ &=\frac{1}{Z}\left\{\lambda_h^+\lambda_c^+(\lambda_h^-+\lambda_c^-)\left[\beta_c\left(g-\frac{\omega_0}{2}+\epsilon\right)-\beta_h\left(g+\frac{\omega_0}{2}+\epsilon\right)\right](n_h^+-n_c^+)+\lambda_h^-\lambda_c^-(\lambda_h^++\lambda_c^+)\right.\\ &\left.\times\left[\beta_c\left(g-\frac{\omega_0}{2}-\epsilon\right)-\beta_h\left(g+\frac{\omega_0}{2}-\epsilon\right)\right](n_h^--n_c^-)\right\},\end{aligned} \tag{7.9}$$

as well as the steady-state efficiency, $\eta^{ss}$

$$\eta^{ss}=-\frac{\mathscr{P}^{ss}}{\mathscr{Q}_h^{ss}}\frac{\omega_0}{g+\frac{\omega_0}{2}+\epsilon\dfrac{\lambda_h^+\lambda_c^+(\lambda_h^-+\lambda_c^-)(n_h^+-n_c^+)-\lambda_h^-\lambda_c^-(\lambda_h^++\lambda_c^+)(n_h^--n_c^-)}{\lambda_h^+\lambda_c^+(\lambda_h^-+\lambda_c^-)(n_h^+-n_c^+)+\lambda_h^-\lambda_c^-(\lambda_h^++\lambda_c^+)(n_h^--n_c^-)}}. \tag{7.10}$$

Since the reduced density operator of the working medium does not change in steady-state, the rate of entropy production in Eq. 7.9 only accounts for the entropy produced in the baths due to heat exchange. Recalling the definitions of $n_i^{\pm}$ in Eqs. 7.2 and 7.4, the steady-state rate of entropy production becomes non-negative, i.e. $\dot{\Sigma}^{ss}\geqslant 0$. Hence, the second law of thermodynamics is satisfied by the generalized Lamb equations even under very intense driving fields.

We emphasize that the second law is satisfied irrespective of the specific realization of the heat baths. Furthermore,

the steady-state efficiency is dependent on the driving field contrary to that obtained from the standard Lamb equations. Since the second law is satisfied, an upper limit of the Carnot efficiency is automatically imposed on this efficiency in the heat engine mode of operation. The specific dependence of the efficiency $\eta^{ss}$ upon $\epsilon$ depends on a specific realization of the bath. Thus no general statement can be made with regard to the specific dependence of $\eta^{ss}$ upon $\epsilon$, except at certain limits discussed below.

Perhaps the most striking observation is that under very intense fields the power (Eq. 7.5) eventually *decreases* as a function of the driving fields intensity, rather than saturate as predicted by the standard Lamb equations (cf. Eq. A3). It is also known that the generalized Lamb equations coincides with the standard ones at weak fields where the power monotonically *increases* as a function of the driving fields intensity (cf. Secs. V, VI and Appendix A). As a consequence the power has a maximum as a function of the field amplitude! This result is qualitatively similar to the analogous result in the low-frequency regime,[18] although the underlying mechanism is quite different.

In order to understand the microscopic mechanism that keeps the second law intact and shapes the maximum in power as a function of the fields intensity, the splitting of the engine to the upper and lower manifolds of Sec. VII A is reexamined. The numerator in each of the expressions for the power and heat flows in Eqs. 7.5–7.7 consists of a sum of two contributions: one, which is proportional to $n_h^+ - n_c^+$, is associated with the population inversion in the upper manifold, while the other, which is proportional to $n_h^- - n_c^-$, is associated with the population inversion in the lower manifold (also cf. Eq. A7). Although the coefficients of these population inversion terms mix parameters associated with both manifolds, it is helpful to think of them as associated with two separate amplifiers. Their relative contribution to the total rate of energy exchange is proportional to the relative sizes of the population inversion terms.

The power reaches a maximum as a function of field intensity $\epsilon$ because of a competition between the upper and lower manifolds. As $\epsilon$ *increases*, the population difference of the upper manifold $n_h^+ - n_c^+$ *increases*, whereas $n_h^- - n_c^-$ of the lower manifold *decreases*. Hence, the power production of the upper manifold *increases*, whereas that of the lower manifold *decreases*. The net power decreases, i.e. the net rate of operation decreases, because as $\epsilon$ increases, a larger portion of the three-level atoms occupy the lower manifold at the expense of the upper one (i.e. $\hat{\Pi}_l$ increases at the expense of $\hat{\Pi}_u$, cf. Eqs. 7.1 and 7.3). Summarizing, the population difference $n_h^+ - n_c^+$ becomes smaller while $n_h^- - n_c^-$ becomes larger.

From a thermodynamic point of view, each manifold is associated with a separate heat engine. As the coupling with the work reservoir ($\epsilon$) increases, the engine associated with the upper manifold operates *faster* while that associated with the lower one operates *slower*, and working fluid is leaking from the former to the latter, thereby diminishing the net power production. We are not aware of a similar loss mechanism in classical macroscopic engines.

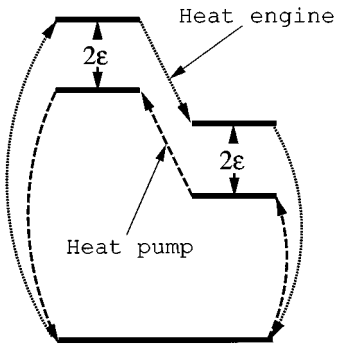


FIG. 4. The two manifolds operate in opposite directions in the vicinity of $\epsilon = \epsilon_{\max}$. The net power vanishes when the two manifolds are exactly balanced.

Not only does the power decrease as a function of $\epsilon$, it also changes sign at a certain *finite* value of the field amplitude, denoted by $\epsilon_{\max}$. This results from the fact that at some point the lower manifold starts operating backwards as a heat pump. At $\epsilon = \epsilon_{\max}$, the power *consumption* by the lower manifold is exactly balanced by the power *production* of the upper manifold, such that the *net* power production is zero (cf. Fig 4).

An examination of the steady-state heat fluxes, Eqs. 7.6 and 7.7, reveals that they do *not* vanish at zero-power operating conditions. Although both manifolds operate at the same rate and in opposite directions, the upper manifold absorbs more heat from the hot bath than that rejected by the lower one. Similarly, the upper manifold rejects more heat into the cold bath than that absorbed by the lower one. The net heat absorbed from the hot bath and rejected into the cold bath in zero-power operating conditions is therefore proportional to the difference in the energy gaps associated with these transitions, i.e. proportional to $2\epsilon$ (cf. Fig. 4). Thus, zero-power operating conditions generally correspond to the short circuit limit, rather than the reversible limit, where heat is effectively transferred *from* the hot bath *into* the cold bath, such that no net work is involved. This fact should be contrasted with the high field performance in the low frequency regime, where only one manifold exists, and hence zero power corresponds to reversible operation.[21]

An interesting limit is that of low temperatures, such that $\epsilon \gg T_c, T_h$. In such a case $n_h^+ - n_c^+$ is negligible relative to $n_h^- - n_c^-$, and only the lower manifold needs be accounted for. The efficiency, Eq. 7.10, then simplifies to

$$\eta_{lT} = \frac{\omega_0}{g + \omega_0/2 - \epsilon}, \tag{7.11}$$

which is the quotient of the energy quanta associated with the coupling to the work and hot baths. Thus the efficiency in this case monotonically *increases* as a function of $\epsilon$.

The value of $\epsilon_{\max}$ in this limit, denoted by $\epsilon_{\max}^{lT}$, is that for which $n_h^- - n_c^- = 0$. It is generally given by:

$$\epsilon_{\max}^{lT}=\frac{\beta_c(g-\omega_0/2)-\beta_h(g+\omega_0/2)}{\beta_c-\beta_h}. \tag{7.12}$$

The condition $\beta_c(g-\omega_0/2)-\beta_h(g+\omega_0/2)>0$ is necessary and sufficient for lasing in the limit of weak driving fields (cf. Appendix A). Since the low-temperature limit only accounts for the lower manifold, and since population inversion becomes increasingly more difficult in this manifold as the field intensifies, it is no longer a sufficient condition for lasing in the case of intense driving fields. Finally, zero-power operating conditions in the low-temperature limit, obtained at $\epsilon=\epsilon_{\max}^{lT}$, asymptotically implies zero heat flows and hence the reversible limit. Indeed, substituting $\epsilon_{\max}^{lT}$ from Eq. 7.12 for $\epsilon$ in Eq. 7.11 reduces it to the Carnot efficiency, $1-T_c/T_h$.

The above low-temperature limit has to be carefully analyzed in the close vicinity of zero power operating conditions. The neglect of the upper manifold is unjustified there despite the low temperatures. Strictly, the efficiency must always *vanish* at zero-power operating conditions, rather than approach the Carnot efficiency. This results from the fact that at zero-power (cf. Eq. 7.5),

$$\lambda_h^-\lambda_c^-(\lambda_h^++\lambda_c^+)(n_h^--n_c^-)+\lambda_h^+\lambda_c^+(\lambda_h^-+\lambda_c^-)\times(n_h^+-n_c^+)=0, \tag{7.13}$$

hence,

$$\lambda_h^+\lambda_c^+(\lambda_h^-+\lambda_c^-)(n_h^+-n_c^+)-\lambda_h^-\lambda_c^-(\lambda_h^++\lambda_c^+)(n_h^--n_c^-)=2\lambda_h^+\lambda_c^+(\lambda_h^-+\lambda_c^-)(n_h^+-n_c^+)>0, \tag{7.14}$$

such that the ratio in the denominator of Eq. 7.10 goes to infinity, and hence the efficiency becomes zero. The performance of the amplifier *always* results from an *interplay* between the slower, more efficient, lower manifold and the faster, less efficient, upper manifold. The balance is determined by the relative occupancies, regulated by the bath temperatures. Lower bath temperatures would indeed favor the slower, more efficient lower manifold and will allow for a closer approach to the maximum Carnot efficiency. However, whereas the lower manifold eventually slows down to a stand still, the upper manifold does not. It then compensates for the lack of occupancy by speed and eventually reduces the efficiency to zero.

## VIII. REFRIGERATION AND THE BEHAVIOR AT THE ABSOLUTE ZERO

Like any heat engine the three-level amplifier can be operated in reverse as a heat pump. This mode of operation would imply that heat is being transferred against the temperature gradient from the *cold* bath ($\dot{Q}_c^{ss}>0$) into the *hot* bath ($\dot{Q}_h^{ss}<0$) by the investment of work ($\mathcal{P}^{ss}>0$).

In the weak-field treatment based on the standard Lamb equations, refrigeration is obtained provided the inequality $\exp[-\beta_h(E_u-E_g)]<\exp[-\beta_c(E_l-E_g)]$ is satisfied (cf. Appendix A). In such a situation $P_u^{ss}<P_l^{ss}$ (i.e. negative population inversion) and radiation is absorbed from the field. However, this refrigeration strategy has a built in lower bound for the cold bath temperature where cooling is possible: $T_c>T_c^*$, where $T_c^*=T_h(E_l-E_g)/(E_u-E_g)$. At $T_c=T_c^*$ there is equal population in the upper levels $P_u^{ss}=P_l^{ss}$ which leads to vanishingly slow operation, i.e. a reversible limit (cf. Refs. 47–51). As the cold bath temperature falls below $T_c^*$, population inversion is created and the device changes into an amplifier, i.e. a heat engine.

Could the refrigeration proceed at lower values of $T_c$, perhaps even down to the absolute zero, by the use of intense driving fields? This question is first examined in the domain of low temperatures where only the lower manifold is effective (cf. Sec. VII B). Consider a case where $\exp[-\beta_h(g+\omega_0/2)]>\exp[-\beta_c(g-\omega_0/2)]$, such that refrigeration *cannot* be obtained within the framework of the standard Lamb equations. From the results of Sec. VII B we know that the device would operate as a heat engine within the following range of field amplitudes: $(0,\epsilon_{\max}^{lT})$, where $\epsilon_{\max}^{lT}$ is as given in Eq. 7.12. At $\epsilon>\epsilon_{\max}^{lT}$ the device goes through three ''phases'' as a function of $\epsilon$, each of which corresponding to a different mode of operation. These phases are listed in Table VI. The significance of these modes of operation in relation to the position of the energy levels of the lower manifold is schematically shown in Fig. 5.

TABLE VI. Different modes of operation of the three-level amplifier for different ranges of the field amplitude in the low-temperature limit. The sign of $\mathcal{P}^{ss}$, $\dot{Q}_h^{ss}$ and $\dot{Q}_c^{ss}$ is indicated in the designated columns.

| | $\epsilon$ interval | $\mathcal{P}^{ss}$ | $\dot{Q}_h^{ss}$ | $\dot{Q}_c^{ss}$ | Modes of operation |
|---|---|---|---|---|---|
| I | $(0,\epsilon_{\max}^{lT})$ | - | + | - | heat engine |
| II | $(\epsilon_{\max}^{lT},g-\omega_0/2)$ | + | - | + | heat pump |
| III | $(g-\omega_0/2,g+\omega_0/2)$ | + | - | - | pure dissipation |
| IV | $(g+\omega_0/2,\infty)$ | + | + | - | dissipation + heat transfer |

The second $\epsilon$ interval, $(\epsilon_{\max}^{lT},g-\omega_0/2)$, corresponds to a *refrigeration window*. It allows for refrigeration at $T_c<T_c^*$ down to the absolute zero. At absolute zero, $T_c\to 0$, $\epsilon_{\max}^{lT}$ coincides with $g-\omega_0/2$, thereby closing the refrigeration

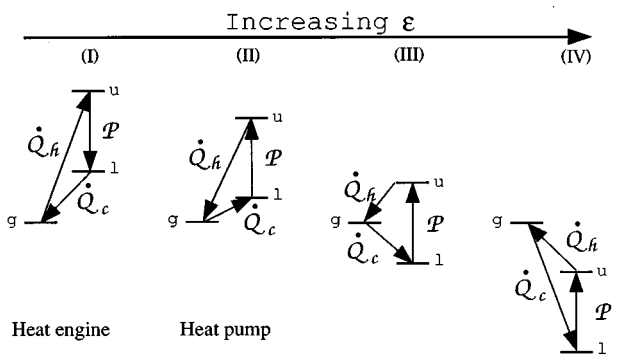


FIG. 5. Different modes of operation of the three-level amplifier for different ranges of the field amplitude in the low-temperature limit. Only the lower manifold, which is dominant in this limit, is shown.

window (cf. Eq. 7.12). Thus the *rate* of pumping heat *out* of the cold bath approaches zero as its temperature approaches absolute zero.

The present derivation of the quantum master equation assumes weak coupling to the baths, implying that they maintain a constant thermal equilibrium. However, in any realization of the bath the internal energy will change in the course of time due to heat exchange. Furthermore, the fast decay of the bath correlations would imply quick thermalization such that the state of the bath can be solely described by its time-dependent temperature. Provided that the change in the bath temperature is slow on the time scale of the bath-induced system's relaxation, which is evident if the bath is very large, the quantum master equation derived here remains valid in the case of baths with time-dependent temperatures. Thus the above refrigeration scheme can be used for cooling the bath degrees of freedom down to absolute zero. As was noted before, refrigeration at such low temperatures is impossible unless the explicit field dependence of the relaxation terms is accounted for.

The above discussion with regard to asymptotic limits associated with the absolute zero is reminiscent of the third law of thermodynamics. The common definition by Nernst's theorem takes the *static* point of view which reads: *The entropy of any system vanishes at the absolute zero temperature*.[54,55] Put in *dynamical* terms this statement may be extended to imply that the *maximum rate* of pumping entropy *out* of a bath continuously approach zero as the bath temperature approaches absolute zero. It was already shown that the refrigeration window closes at absolute zero, such that the maximum rate of pumping heat from the cold bath approaches zero in this limit. The same is true for the maximum rate of entropy pumping, $\dot{\mathcal{Q}}_c^{ss}/T_c$, which is proportional to $n_c^-/T_c$ at the vicinity of absolute zero and hence goes to zero as the absolute zero is approached from above (cf. Eq. 7.7).

A word of caution regarding the application of the theory to low temperature heat baths is however appropriate at this point. At low temperatures, the decay of the bath correlations which occur on time scales of the order of $T$ becomes slower. At the same time, the system's relaxation slows down as well. Both processes comes to a standstill at the absolute zero. Thus, the separation of time scales between the bath and the system becomes questionable at very low temperatures, although it may still hold arbitrarily close to the absolute zero.

Following the refrigeration window are two other modes of operation. Within the third $\epsilon$ interval, III, the dressed level of the lower manifold, denoted $l$, drops *below* the original ground state, denoted $g$, while the dressed level denoted $u$ remains above the original ground state. Hence, the work absorbed from the driving field is completely dissipated into heat which is rejected into both heat baths. One may use $\epsilon$ in order to control the branching ratio by which the total heat is allocated between the two baths. In the last mode of operation, interval IV, both levels $u$ and $l$ lie *below* the original ground state. This operation mode is a mirror image of the heat engine mode in interval I. Heat engine action would result if the couplings with the hot and cold baths were switched. However, within the present setup, heat is rejected into the cold bath which consists of the dissipated work and heat intake from the hot bath.

Beyond the low-temperature limit one must account for the upper manifold as well as for the lower one. The necessary and sufficient condition for refrigeration, i.e. for $\dot{\mathcal{Q}}_c>0$, is then given by (cf. Eq. 7.7):

$$\left(g-\frac{\omega_0}{2}+\epsilon\right)\lambda_h^+\lambda_c^+(\lambda_h^-+\lambda_c^-)(n_h^+-n_c^+)$$

$$+\left(g-\frac{\omega_0}{2}-\epsilon\right)\lambda_h^-\lambda_c^-(\lambda_h^++\lambda_c^+)(n_h^--n_c^-)<0. \qquad (8.1)$$

At the domain of interest, $\epsilon>\epsilon_{\max}$, $n_h^--n_c^-<0$ and $n_h^+-n_c^+>0$. The first term in Eq. 8.1 is therefore positive, and the factors $(g-\omega_0/2+\epsilon)$ and $n_h^+-n_c^+$ *increase* as functions of $\epsilon$. The third factor, $\lambda_h^+\lambda_c^+(\lambda_h^-+\lambda_c^-)$, contains an additional dependence upon $\epsilon$ which cannot be specified unless a specific model is assumed for the bath. The second term in Eq. 8.1 is negative provided $\epsilon<g-\omega_0/2$. Hence, to obtain refrigeration, the second term must dominate the first one within the $\epsilon$ interval $(\epsilon_{\max},g-\omega_0/2)$. It should be noted that the contribution of the second term also diminishes as $\epsilon$ approaches $g-\omega_0/2$. Thus, unless the second term dominates in the vicinity of $\epsilon_{\max}$, corresponding to the low-temperature limit, a refrigeration window would not open. It may then be concluded that the refrigeration window is closed at both high and low values of $T_c$, although for different reasons. Thus refrigeration is only obtainable within a narrow domain of the $(T_c,\epsilon)$ plane.

## IX. AN ILLUSTRATIVE SPECIAL CASE

The generalized Lamb equations, Eqs. 4.3 and 4.4, were derived without explicitly specifying the baths. The physical nature of the latter is hidden inside the bath parameters of Table I. Thus all the observations made in previous sections are general and apply to *any* realization of the baths. However, in order to further explore the implications of the generalized Lamb equations, a specific bath model has to be chosen.

In this section the generalized Lamb equations are illustrated in the case of *white baths*. These baths have a *constant* mode density in the frequency range of interest. Modeling the heat baths as white implies that $\lambda_h^{\pm}\to\lambda_h$ and $\lambda_c^{\pm}\to\lambda_c$ with $\lambda_h$ and $\lambda_c$ being *constant*. Other simplifications introduced are: resonance conditions ($|\Delta\omega|\ll|2\epsilon|$) and lack of diagonal couplings with the baths ($\delta_i^1,\delta_i^1,\delta_i^0=0$). Both assumptions generally hold at very intense fields. Emphasis is laid upon the optimization of power with respect to various controls in the spirit of finite-time thermodynamics.

### A. The optimal matching of relaxation rates

Imposing the white bath assumption upon the steady-state power in Eq. 7.5 one obtains:

$$\mathscr{P}_w^{ss} = -\frac{\omega_0 W[(P^0_{u+}-P^0_{l+})+(P^0_{u-}-P^0_{l-})]}{1+\dfrac{W}{\dfrac{\lambda^2-(\delta\lambda)^2}{2\lambda}}+\dfrac{2\delta\lambda}{\lambda^2-(\delta\lambda)^2}W[(P^0_{u+}-P^0_{l+})+(P^0_{u-}-P^0_{l-})]}, \tag{9.1}$$

where $\lambda=(\lambda_h+\lambda_c)/2$, $\delta\lambda=(\lambda_h-\lambda_c)/2$, $W=2\epsilon^2/\lambda$, $P^0_{u\pm}=n_h^{\pm}/(2+n_h^{+}+n_h^{-}+n_c^{+}+n_c^{-})$, and $P^0_{l\pm}=n_c^{\pm}/(2+n_h^{+}+n_h^{-}+n_c^{+}+n_c^{-})$. The occupancies at the levels involved in lasing are normally very small within the heat engine mode of operation such that $P^0_{u\pm},P^0_{l\pm}\ll 1$. Hence, the third term on the denominator on the right hand side of Eq. 9.1 is negligible. It then follows that the power production could be maximized provided that $\delta\lambda=0$, i.e. if the relaxation rates induced by the two baths are *matched*. These matching conditions are assumed from this point on, such that $\lambda_h^{\pm}=\lambda_c^{\pm}=\lambda$.

In both the standard and generalized Lamb equations the power has a maximum as a function of $\lambda$ due to the interplay between population relaxation and dephasing.[18] A simple extension of the model is obtained by adding ''pure dephasing terms'' within a white bath framework, such that $\delta_h^1=\delta_c^1=\delta^1$, where $\delta^1$ is *fixed*. The latter turns out only to affect $W$, which turns into $W=2\epsilon^2/[\lambda+(2\delta^1+\delta_h^1+\delta_c^1)/16]$. Hence, before it is suppressed by the field, the diagonal coupling to the baths simply enhances the rate of dephasing.

### B. Optimization with respect to the field amplitude

Imposing the assumption of *matched* white baths yields the following expressions for the steady-state power and heat fluxes (cf. Eqs. 7.5–7.7):

$$\mathscr{P}_w^{ss} = -\omega_0 W\frac{(P^0_{u+}-P^0_{l+})+(P^0_{u-}-P^0_{l-})}{1+\dfrac{W}{\lambda/2}}, \tag{9.2}$$

$$\mathscr{Q}_{h,w}^{ss} = \left(g+\frac{\omega_0}{2}+\epsilon+\frac{\lambda^2}{4\epsilon}\right)W\frac{P^0_{u+}-P^0_{l+}}{1+\dfrac{W}{\lambda/2}} + \left(g+\frac{\omega_0}{2}-\epsilon-\frac{\lambda^2}{4\epsilon}\right)W\frac{P^0_{u-}-P^0_{l-}}{1+\dfrac{W}{\lambda/2}}, \tag{9.3}$$

$$\mathscr{Q}_{c,w}^{ss} = -\left(g-\frac{\omega_0}{2}+\epsilon+\frac{\lambda^2}{4\epsilon}\right)W\frac{P^0_{u+}-P^0_{l+}}{1+\dfrac{W}{\lambda/2}} - \left(g-\frac{\omega_0}{2}-\epsilon-\frac{\lambda^2}{4\epsilon}\right)W\frac{P^0_{u-}-P^0_{l-}}{1+\dfrac{W}{\lambda/2}}. \tag{9.4}$$

As a consistency check, note that the first law of thermodynamics is satisfied such that $\dot{\mathscr{Q}}_{h,w}^{ss}+\dot{\mathscr{Q}}_{c,w}^{ss}+\mathscr{P}_w^{ss}=0$.

The $\lambda^2/(4\epsilon)$ term in the expressions for the heat fluxes may be neglected by the following argument. For weak fields such that $\epsilon\sim\lambda$, this term is of the order of magnitude of $\epsilon$ (or $\lambda$). Hence it is negligible either assuming high frequency (i.e. $\omega\approx\omega_0\gg\lambda$) or assuming the weak coupling limit ($\epsilon\ll\omega_0$). In this limit $g\pm\omega_0/2\pm\epsilon\pm\lambda^2/(4\epsilon)\to g\pm\omega_0/2$ such that the generalized Lamb equations coincide with the standard ones. As $\epsilon$ increases to become greater than $\lambda$, $\lambda^2/(4\epsilon)$ is further diminished, hence its neglect relative to the remaining $\epsilon$ is consistent.

The steady-state power, heat flows and rate of entropy production obtained within this model are plotted as functions of $\epsilon$ for various temperatures in Figs. 6–7. The power

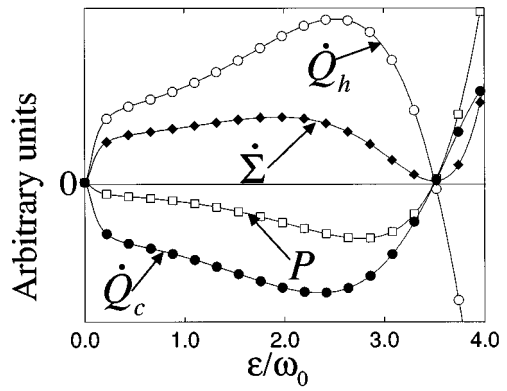


FIG. 6. The steady-state power and rates of heat flow and entropy production as a function of the field amplitude, at the low-temperature domain. This plot was generated for the case of matched white baths with the parameters $\Delta\omega=0$, $g=5\omega_0$, $\lambda=0.2\omega_0$, $T_c=0.5\omega_0$, $T_h=\omega_0$.

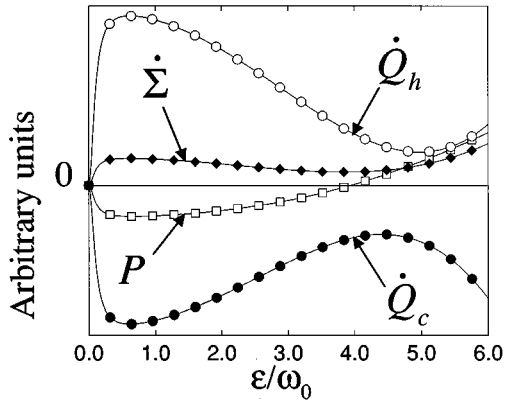


FIG. 7. The steady-state power and rates of heat flow and entropy production as a function of the field amplitude at high temperatures. This plot was generated for the case of white matched baths with the parameters $\Delta\omega=0$, $g=5\omega_0$, $\lambda=0.2\omega_0$, $T_c=2\omega_0$, $T_h=4\omega_0$.

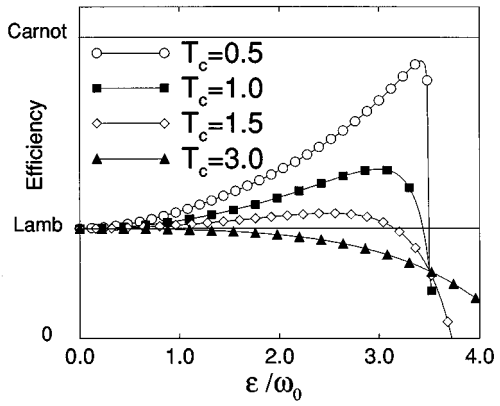


FIG. 8. The efficiency of the amplifier as a function of the amplitude of the field. Different curves correspond to different values of $T_c$, while the temperature ratio is kept fixed, $T_c/T_h=0.5$. Also indicated are the Carnot efficiency and the fixed efficiency predicted by the standard Lamb equations, $\eta_{\mathrm{Lamb}}=\omega_0/(g+\omega_0/2)$. This plot was generated for the parameters $\lambda=0.2\omega_0$, $g=5\omega_0$.

production goes through a maximum and then decrease. The sign convention is that the power *production* has the reverse sign of the power *exchange*, which is plotted in Figs. 6 and 7. Thus, negative values for the power in the plots correspond to positive power production by the engine. Fig. 6 corresponds to sufficiently *low* temperatures such that $\epsilon_{\max}\gg T_c, T_h$. Hence, the lower manifold dominates in the vicinity of zero-power operating conditions. All fluxes go to zero when the power does, thereby signaling *reversible operation*. In Fig. 7, the temperatures are high enough such that both manifolds are still active when the power switches sign. At zero-power operating conditions the power production by the *upper* manifold is exactly balanced by the power consumption of the *lower* manifold, however heat is being constantly absorbed from the hot bath and transmitted into the cold one. (cf. Fig. 4). The non-negligible operation of the upper manifold also pushes $\epsilon_{\max}$ to higher values, as a comparison of Fig. 6 with Fig. 7 reveals.

The steady-state efficiency provides a different angle for examining the irreversible nature of the amplifiers' operation. Imposing the assumption of matched white baths upon Eq. 7.10, the following expression is obtained for the steady-state efficiency:

$$\eta_w^{ss}=\frac{\omega_0}{g+\frac{\omega_0}{2}+\left(\epsilon+\frac{\lambda^2}{4\epsilon}\right)\frac{(P_{u+}^0-P_{l+}^0)-(P_{u-}^0-P_{l-}^0)}{(P_{u+}^0-P_{l+}^0)+(P_{u-}^0-P_{l-}^0)}}. \tag{9.5}$$

Fig. 8 shows the efficiency of the amplifier as a function of the field amplitude for various bath temperatures. All curves correspond to the same value of $T_c/T_h$ and hence to the same Carnot efficiency. As was already noted, the efficiency universally decreases to zero at zero-power operating conditions. However, rather than monotonically decrease to zero it may go through a maximum that approaches the Carnot efficiency as the temperatures decrease.

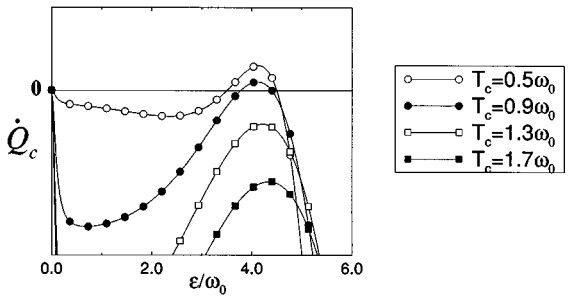


FIG. 10. $\dot{Q}_c$ as a function of $\epsilon$ for several high temperatures. The closing of the refrigeration window as the temperature *increases*, due to the upper manifold, is clearly seen. This plot was generated for the parameters $\lambda=0.2\omega_0$, $g=5\omega_0$, $T_c/T_h=0.5$.

### C. Refrigeration and Other Modes of Operation

The four modes of operation available at the low-temperature limit are demonstrated in Fig. 9 for the case of matched white baths (cf. Table VI). A refrigeration window is opened at the interval II. The closing of the refrigeration window as the temperatures *increase* is shown in Fig. 10. The latter results from the fact that the upper manifold is still

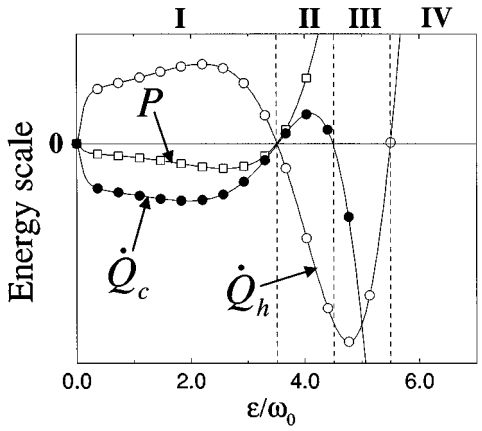


FIG. 9. The four modes of operation at the low-temperature limit. A refrigeration window is opened at interval II. This plot was generated for the parameters $\lambda=0.2\omega_0$, $g=5\omega_0$, $T_c=0.6\omega_0$, $T_h=1.2\omega_0$.

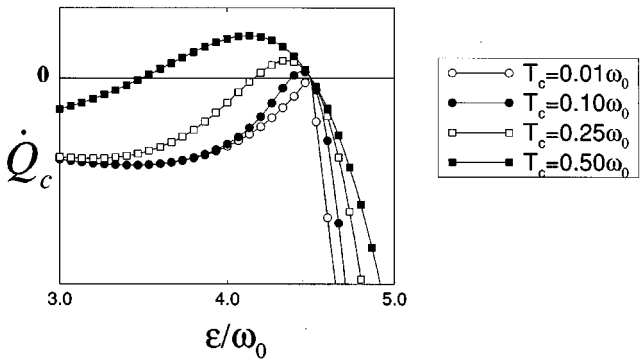


FIG. 11. $\dot{Q}_c$ as a function of $\epsilon$ at low temperatures. The closing of the refrigeration window as the temperature *decreases* is clearly seen. This plot was generated for the parameters $\lambda=0.2\omega_0$, $g=5\omega_0$, $T_c/T_h=0.5$.

effective at high temperatures (cf. Sec. VIII). The complementary closing of the refrigeration window at *low* temperatures is shown in Fig. 11.

## X. SUMMARY

The main results of the present study may be be summarized as follows:

- Generalized Lamb equations for a three-level quantum amplifier operated in the *high-frequency* regime were derived from first principles. These generalized Lamb equations are applicable at *any* field intensity and for a very general coupling scheme with the baths. We are not aware of any previous attempt to derive these equations.
- The generalized Lamb equations were shown to be consistent with the second law of thermodynamics at domains where it is not satisfied by the standard Lamb equations. We are not aware of any previous demonstration of the second law of thermodynamics for a dissipative quantum system driven by a *strong* field (except for Ref. 19).
- The standard Lamb equations were shown to coincide with the generalized Lamb equations in the limit of weak fields and/or far from resonance. Thus the limitations of the standard Lamb equations were clarified, and the deviations from them, once they cease to be valid, pointed out.
- The relaxation terms in the generalized Lamb equations were shown to induce relaxation of the field-dressed atom rather than the bare atom. This holds true in general for systems driven by a rapidly rotating field.
- It was demonstrated that, similar to the generalized Bloch equations, the *diagonal* coupling terms with the baths are completely suppressed by strong driving fields.
- The steady-state operation of the amplifier was studied in detail in the domain of very intense driving fields. The steady-state power was shown to go through a maximum and eventually switch sign, unlike in the standard treatment where it saturates. Zero-power operation was shown to result from a balance between two dressed three-level manifolds, one operating as a heat engine and the other as a heat pump. The efficiency of the amplifier was shown to have a maximum as a function of the field amplitude, which approaches the Carnot efficiency as the bath temperatures decrease.
- A refrigeration window was shown to exist at very high field intensities which allows for refrigeration at values of $T_c$ lower than the lower bound set by the standard weak field treatment. Such a refrigeration procedure may proceed down to absolute zero, where the window is closed. It was suggested that the closing of the refrigeration window at absolute zero is a *dynamical* manifestation to the third law of thermodynamics.
- An application of the generalized Lamb equations for a three-level amplifier coupled to white baths was considered. Matching the relaxation rates of the baths was shown to be the favorable choice if the maximization of power is desirable. All general results were demonstrated and confirmed for this example.

Throughout this paper the performance of the amplifier was considered with the Rabi frequency, $\epsilon$, as a control. The intensity of the driving field was defined by the size of $\epsilon$ relative to other parameters. The Rabi frequency is explicitly given by $\epsilon = -\vec{\mu}\cdot\vec{E}_0$, where $\vec{\mu}$ is the transition dipole moment and $\vec{E}_0$ the actual amplitude of the driving field. As was recently pointed out by Evans *et al.*,[56] values of $\epsilon/\omega_0 \sim 1$ are experimentally accessible by existing light sources in cases involving charge separation over a distance of several Angstroms, and are unlikely to result in dielectric breakdown of the solvent on the time scale required to arrive at steady-state.

A very attractive possible extension of the present work is to apply thermodynamic reasoning to the analysis of laser cooling experiments.[57–60] Although its name suggests otherwise, present theoretical models of laser cooling are mostly mechanistic rather than thermodynamic. To see how such thermodynamic thinking may be invoked, consider the case of Doppler cooling. The pumping lasers may be taken to be the work reservoir, the rest of the modes of the radiation field into which spontaneous emission is rejected the hot bath, and the atomic translational degrees of freedom which are cooled as the cold bath. The resulting setup is reminiscent of the three-level amplifier when its operation is reversed. At present the lowest temperature to which the translation can be cooled seems to be bounded from below. We hypothesize that this lower bound is similar to $T_c^*$ imposed by the standard Lamb equations which is due to the use of relatively low intensity laser light. If this is so, could one attain even lower temperatures by operating inside the refrigeration window opened at higher fields (cf. Sec. VIII)? We intend to explore this and related intriguing questions in the future.

## ACKNOWLEDGMENTS

We thank David Tannor, Jim Skinner and Allon Bartana for helpful discussions. Partially supported by the Israel science foundation and the U.S. Navy under contract No. N00014-91J1498. The Fritz Haber Research Center is supported by the Minerva Gesellschaft für die Forschung, GmbH München, FRG.

## APPENDIX A: THE STANDARD LAMB EQUATIONS

The standard Lamb equations are obtained in the limit of weak coupling to both the bath *and* the driving field. This implies that the two levels coupled to the hot bath, $|g\rangle$ and $|u\rangle$, are relaxed by one field-free standard Bloch-like equation,[19] whereas the two levels coupled to the cold bath, $|g\rangle$ and $|l\rangle$, are relaxed by another. Note however that the population in each of these ''two-level systems'' is not con-

served in contrast to the standard Bloch equations, namely $P_u+P_g \neq 1$ and $P_l+P_g \neq 1$. The driving field term only enters via the Hamiltonian contribution to the dynamics. The equations of motion in the rotating frame become:

$$\frac{d}{dt}\begin{bmatrix}\hat{\mathbf{P}}_+\\ \hat{\mathbf{P}}_-\\ \hat{\mathbf{P}}_\mathbf{u}\\ \hat{\mathbf{P}}_\mathbf{l}\end{bmatrix}=\begin{bmatrix} i\Delta\omega-\Gamma_d & 0 & -i\epsilon & i\epsilon\\ 0 & -i\Delta\omega-\Gamma_d & i\epsilon & -i\epsilon\\ -i\epsilon & i\epsilon & -(\lambda_h^0+\overline{\lambda_h^0}) & -\overline{\lambda_h^0}\\ i\epsilon & -i\epsilon & -\overline{\lambda_c^0} & -(\lambda_c^0+\overline{\lambda_c^0})\end{bmatrix}\begin{bmatrix}\hat{\mathbf{P}}_+\\ \hat{\mathbf{P}}_-\\ \hat{\mathbf{P}}_\mathbf{u}\\ \hat{\mathbf{P}}_\mathbf{l}\end{bmatrix}+\begin{bmatrix}0\\ 0\\ \overline{\lambda_h^0}\\ \overline{\lambda_c^0}\end{bmatrix}. \tag{A1}$$

Here, $\hat{\mathbf{P}}_+=|u\rangle\langle l|\exp(i\omega t)$ and $\hat{\mathbf{P}}_-=|l\rangle\langle u|\exp(-i\omega t)$ are the creation and annihilation operators corresponding to the lasing transition in the rotating frame; $\hat{\mathbf{P}}_\mathbf{l}=|l\rangle\langle l|$ and $\hat{\mathbf{P}}_\mathbf{u}=|u\rangle\langle u|$ are the projectors onto the two upper states; $\Delta\omega=E_u-E_l-\omega$ is the detuning; $\Gamma_d=\frac{1}{2}(\lambda_h^0+\lambda_c^0)+\frac{1}{8}(\delta_h^0+\delta_c^0)$ is the dephasing rate; and finally,

$$\begin{aligned}&\lambda_h^0=\widetilde{C}^h_{\Lambda\Lambda^\dagger}(E_u-E_g),\quad \lambda_c^0=\widetilde{C}^c_{\Lambda\Lambda^\dagger}(E_l-E_g),\\ &\overline{\lambda_h^0}=\lambda_h^0 e^{-\beta_h(E_u-E_g)},\quad \overline{\lambda_c^0}=\lambda_c^0 e^{-\beta_c(E_l-E_g)},\\ &\delta_h^0=\widetilde{C}^h_{\Delta\Delta}(0),\quad \delta_c^0=\widetilde{C}^c_{\Delta\Delta}(0)\end{aligned} \tag{A2}$$

are the relaxation and pure dephasing coefficients (cf. Eqs. 3.3 and 3.4).

Solving Eq. A1 for steady-state, the following expressions are obtained for the power and heat flows (cf. Eqs. 1.3 and 1.4):

$$\mathscr{P}^{ss}_{Lamb}=-\frac{\omega W(P_u^0-P_l^0)}{1+W/\Gamma}, \tag{A3}$$

$$\dot{\mathscr{Q}}^{ss}_{h,Lamb}=\left(E_u-E_g-\Delta\omega\frac{\frac{1}{2}\lambda_h^0+\frac{1}{8}\delta_h^0}{\Gamma_d}\right)\frac{W(P_u^0-P_l^0)}{1+W/\Gamma}, \tag{A4}$$

$$\dot{\mathscr{Q}}^{ss}_{c,Lamb}=-\left(E_l-E_g+\Delta\omega\frac{\frac{1}{2}\lambda_c^0+\frac{1}{8}\delta_c^0}{\Gamma_d}\right)\frac{W(P_u^0-P_l^0)}{1+W/\Gamma}. \tag{A5}$$

Here $W$ is the rate of stimulated emission:

$$W=\frac{2\Gamma_d\epsilon^2}{(\Delta\omega)^2+\Gamma_d^2}; \tag{A6}$$

$P_u^0$ and $P_l^0$ are the population at the energy levels $E_u$ and $E_l$, respectively, in a *field-free* thermal equilibrium,

$$\begin{aligned}P_u^0&=\frac{\overline{\lambda_h^0}\lambda_c^0}{\lambda_h^0\lambda_c^0+\lambda_h^0\lambda_c^0+\lambda_h^0\lambda_c^0}\\ &=\frac{e^{-\beta_h(E_u-E_g)}}{1+e^{-\beta_h(E_u-E_g)}+e^{-\beta_c(E_l-E_g)}},\end{aligned}$$

$$\begin{aligned}P_l^0&=\frac{\lambda_h^0\overline{\lambda_c^0}}{\lambda_h^0\lambda_c^0+\lambda_h^0\lambda_c^0+\lambda_h^0\lambda_c^0}\\ &=\frac{e^{-\beta_c(E_l-E_g)}}{1+e^{-\beta_h(E_u-E_g)}+e^{-\beta_c(E_l-E_g)}};\end{aligned} \tag{A7}$$

and,

$$\Gamma=\frac{\lambda_h^0\lambda_c^0+\overline{\lambda_h^0}\lambda_c^0+\lambda_h^0\overline{\lambda_c^0}}{\lambda_h^0+2\lambda_h^0+\lambda_c^0+2\lambda_c^0}. \tag{A8}$$

Consistency with the second law of thermodynamics requires that the rate of entropy production, $\dot{\Sigma}=-\beta_h\dot{\mathscr{Q}}_h-\beta_c\dot{\mathscr{Q}}_c$, be non-negative. However, the $\Delta\omega$-dependent term in the heat flows introduces an unbounded contribution to the entropy production that may lead to negative values. Hence, the Lamb equations are not thermodynamically consistent. The source of this inconsistency can be traced back to the fact that the structure of the Hamiltonian of the working medium is built into the dissipation super-operator via the detailed-balance relations and the eigen-projection operators.[19] The standard Lamb equations only relax the field-free system, while the real Hamiltonian contains an additional term corresponding to the interaction with the field. The non-physical $\Delta\omega$-dependent terms in Eqs. (1.4) and (1.5) emerge from operating with this field-free generator on this term.

Another non-physical property of the standard Lamb equations reveals itself when the efficiency is considered in resonance. It turns out to be constant, $\eta=(E_u-E_l)/(E_u-E_g)$, i.e. independent of the field. This is unreasonable since the rate of operation is certainly regulated by the field

intensity, leading to a field-dependent degree of irreversibility which should affect the efficiency of the amplifier. Such an effect is indeed detectable once the assumption of weak coupling with the field is abandoned.

The dependence of the steady-state power, Eq. A3, upon the field amplitude, $\epsilon$, should be noted. Only $W$ depends on $\epsilon$ (cf. Eq. 1.6). Thus the power monotonically increases as a function of $\epsilon$ and saturates at high field intensities. The generalized Lamb equations predict a *different* post-saturation behavior, where the power reaches a maximum and eventually decreases and even switches from emission to absorption at high intensities.

## APPENDIX B: THE GENERALIZED QUANTUM MASTER EQUATION FOR THE THREE-LEVEL AMPLIFIER IN THE HIGH-FREQUENCY REGIME

The derivation of the generalized quantum master equation for the three-level amplifier in the high-frequency regime is outlined in Sec. III. The resulting Heisenberg generalized quantum master equation for any observable, $\mathbf{X}$, of the three-level atom is given by:

$$
\begin{aligned}
d\mathbf{X}dt = {} & i[\mathbf{H_s^0}+\mathbf{W}(t),\mathbf{X}]+\frac{\partial}{\partial t}\mathbf{X}+\gamma_1([\hat{\mathbf{\Pi}}_+^{\mathbf{h}},\mathbf{X}]\hat{\mathbf{\Pi}}_-^{\mathbf{h}}+\hat{\mathbf{\Pi}}_+^{\mathbf{h}}[\mathbf{X},\hat{\mathbf{\Pi}}_-^{\mathbf{h}}])+\kappa_1(\hat{\mathbf{\Pi}}_-^{\mathbf{h}}[\mathbf{X},\hat{\mathbf{\Pi}}_+^{\mathbf{h}}]+[\hat{\mathbf{\Pi}}_-^{\mathbf{h}},\mathbf{X}]\hat{\mathbf{\Pi}}_+^{\mathbf{h}})+\gamma_2([\hat{\mathbf{\Pi}}_+^{\mathbf{h}},\mathbf{X}]\hat{\mathbf{\Pi}}_-^{\mathbf{c}} \\
& +\hat{\mathbf{\Pi}}_+^{\mathbf{c}}[\mathbf{X},\hat{\mathbf{\Pi}}_-^{\mathbf{h}}])+\kappa_2(\hat{\mathbf{\Pi}}_-^{\mathbf{c}}[\mathbf{X},\hat{\mathbf{\Pi}}_+^{\mathbf{h}}]+[\hat{\mathbf{\Pi}}_-^{\mathbf{h}},\mathbf{X}]\hat{\mathbf{\Pi}}_+^{\mathbf{c}})+\gamma_3([\hat{\mathbf{\Pi}}_+^{\mathbf{c}},\mathbf{X}]\hat{\mathbf{\Pi}}_-^{\mathbf{h}}+\hat{\mathbf{\Pi}}_+^{\mathbf{h}}[\mathbf{X},\hat{\mathbf{\Pi}}_-^{\mathbf{c}}])+\kappa_3(\hat{\mathbf{\Pi}}_-^{\mathbf{h}}[\mathbf{X},\hat{\mathbf{\Pi}}_+^{\mathbf{c}}]+[\hat{\mathbf{\Pi}}_-^{\mathbf{c}},\mathbf{X}]\hat{\mathbf{\Pi}}_+^{\mathbf{h}}) \\
& +\gamma_4([\hat{\mathbf{\Pi}}_+^{\mathbf{c}},\mathbf{X}]\hat{\mathbf{\Pi}}_-^{\mathbf{c}}+\hat{\mathbf{\Pi}}_+^{\mathbf{c}}[\mathbf{X},\hat{\mathbf{\Pi}}_-^{\mathbf{c}}])+\kappa_4(\hat{\mathbf{\Pi}}_-^{\mathbf{c}}[\mathbf{X},\hat{\mathbf{\Pi}}_+^{\mathbf{c}}]+[\hat{\mathbf{\Pi}}_-^{\mathbf{c}},\mathbf{X}]\hat{\mathbf{\Pi}}_+^{\mathbf{c}})+\gamma_5[\hat{\mathbf{\Pi}}_{\mathbf{z}}^{\mathbf{h}},\mathbf{X}]\hat{\mathbf{\Pi}}_{\mathbf{z}}^{\mathbf{h}}+\kappa_5\hat{\mathbf{\Pi}}_{\mathbf{z}}^{\mathbf{h}}[\mathbf{X},\hat{\mathbf{\Pi}}_{\mathbf{z}}^{\mathbf{h}}]+\gamma_6[\hat{\mathbf{\Pi}}_{\mathbf{z}}^{\mathbf{h}},\mathbf{X}]\hat{\mathbf{\Pi}}_{\mathbf{z}}^{\mathbf{c}} \\
& +\kappa_6\hat{\mathbf{\Pi}}_{\mathbf{z}}^{\mathbf{c}}[\mathbf{X},\hat{\mathbf{\Pi}}_{\mathbf{z}}^{\mathbf{h}}]+\gamma_7[\hat{\mathbf{\Pi}}_{\mathbf{z}}^{\mathbf{c}},\mathbf{X}]\hat{\mathbf{\Pi}}_{\mathbf{z}}^{\mathbf{h}}+\kappa_7\hat{\mathbf{\Pi}}_{\mathbf{z}}^{\mathbf{h}}[\mathbf{X},\hat{\mathbf{\Pi}}_{\mathbf{z}}^{\mathbf{c}}]+\gamma_8[\hat{\mathbf{\Pi}}_{\mathbf{z}}^{\mathbf{c}},\mathbf{X}]\hat{\mathbf{\Pi}}_{\mathbf{z}}^{\mathbf{c}}+\kappa_8\hat{\mathbf{\Pi}}_{\mathbf{z}}^{\mathbf{c}}[\mathbf{X},\hat{\mathbf{\Pi}}_{\mathbf{z}}^{\mathbf{c}}]+\gamma_9([\hat{\mathbf{\Pi}}_+,\mathbf{X}]\hat{\mathbf{\Pi}}_++\hat{\mathbf{\Pi}}_-[\mathbf{X},\hat{\mathbf{\Pi}}_-]) \\
& +\kappa_9(\hat{\mathbf{\Pi}}_+[\mathbf{X},\hat{\mathbf{\Pi}}_+]+[\hat{\mathbf{\Pi}}_-,\mathbf{X}]\hat{\mathbf{\Pi}}_-)+\gamma_{10}([\hat{\mathbf{\Pi}}_+,\mathbf{X}]\hat{\mathbf{\Pi}}_-+\hat{\mathbf{\Pi}}_+[\mathbf{X},\hat{\mathbf{\Pi}}_-])+\kappa_{10}(\hat{\mathbf{\Pi}}_-[\mathbf{X},\hat{\mathbf{\Pi}}_+]+[\hat{\mathbf{\Pi}}_-,\mathbf{X}]\hat{\mathbf{\Pi}}_+) \\
& +\gamma_{11}([\hat{\mathbf{\Pi}}_{\mathbf{z}}^{\mathbf{h}},\mathbf{X}]\hat{\mathbf{\Pi}}_++\hat{\mathbf{\Pi}}_-[\mathbf{X},\hat{\mathbf{\Pi}}_{\mathbf{z}}^{\mathbf{h}}])+\kappa_{11}(\hat{\mathbf{\Pi}}_+[\mathbf{X},\hat{\mathbf{\Pi}}_{\mathbf{z}}^{\mathbf{h}}]+[\hat{\mathbf{\Pi}}_{\mathbf{z}}^{\mathbf{h}},\mathbf{X}]\hat{\mathbf{\Pi}}_-)+\gamma_{12}([\hat{\mathbf{\Pi}}_{\mathbf{z}}^{\mathbf{c}},\mathbf{X}]\hat{\mathbf{\Pi}}_++\hat{\mathbf{\Pi}}_-[\mathbf{X},\hat{\mathbf{\Pi}}_{\mathbf{z}}^{\mathbf{c}}])+\kappa_{12}(\hat{\mathbf{\Pi}}_+[\mathbf{X},\hat{\mathbf{\Pi}}_{\mathbf{z}}^{\mathbf{c}}] \\
& +[\hat{\mathbf{\Pi}}_{\mathbf{z}}^{\mathbf{c}},\mathbf{X}]\hat{\mathbf{\Pi}}_-)+\gamma_{13}([\hat{\mathbf{\Pi}}_+,\mathbf{X}]\hat{\mathbf{\Pi}}_{\mathbf{z}}^{\mathbf{h}}+\hat{\mathbf{\Pi}}_{\mathbf{z}}^{\mathbf{h}}[\mathbf{X},\hat{\mathbf{\Pi}}_-])+\kappa_{13}(\hat{\mathbf{\Pi}}_{\mathbf{z}}^{\mathbf{h}}[\mathbf{X},\hat{\mathbf{\Pi}}_+]+[\hat{\mathbf{\Pi}}_-,\mathbf{X}]\hat{\mathbf{\Pi}}_{\mathbf{z}}^{\mathbf{h}})+\gamma_{14}([\hat{\mathbf{\Pi}}_+,\mathbf{X}]\hat{\mathbf{\Pi}}_{\mathbf{z}}^{\mathbf{c}}+\hat{\mathbf{\Pi}}_{\mathbf{z}}^{\mathbf{c}}[\mathbf{X},\hat{\mathbf{\Pi}}_-]) \\
& +\kappa_{14}(\hat{\mathbf{\Pi}}_{\mathbf{z}}^{\mathbf{c}}[\mathbf{X},\hat{\mathbf{\Pi}}_+]+[\hat{\mathbf{\Pi}}_-,\mathbf{X}]\hat{\mathbf{\Pi}}_{\mathbf{z}}^{\mathbf{c}}). \qquad \text{(B1)}
\end{aligned}
$$

TABLE VII. The relaxation coefficients in the generalized quantum master equation. $c$ and $s$ stand for $\cos\theta$ and $\sin\theta$, respectively, where $\tan\theta = 2\epsilon/\Delta\omega$.

| | | | |
|---|---|---|---|
| $\gamma_1$ | $\frac{1}{4}(1+c)\lambda_h^+ + \frac{1}{4}(1-c)\lambda_c^+$ | $\kappa_1$ | $\frac{1}{4}(1+c)\overline{\lambda_h^+} + \frac{1}{4}(1-c)\overline{\lambda_c^+}$ |
| $\gamma_2$ | $\frac{1}{4}s(-\lambda_h^- + \lambda_c^-)$ | $\kappa_2$ | $\frac{1}{4}s(-\overline{\lambda_h^-} + \overline{\lambda_c^-})$ |
| $\gamma_3$ | $\frac{1}{4}s(-\lambda_h^+ + \lambda_c^+)$ | $\kappa_3$ | $\frac{1}{4}s(-\overline{\lambda_h^+} + \overline{\lambda_c^+})$ |
| $\gamma_4$ | $\frac{1}{4}(1-c)\lambda_h^- + \frac{1}{4}(1+c)\lambda_c^-$ | $\kappa_4$ | $\frac{1}{4}(1-c)\overline{\lambda_h^-} + \frac{1}{4}(1+c)\overline{\lambda_c^-}$ |
| $\gamma_5 = \kappa_5$ | | | $\frac{1}{8}(1+c)^2\delta_h^0 + \frac{1}{8}(1-c)^2\delta_c^0$ |
| $\gamma_6 = \kappa_6 = \gamma_7 = \kappa_7$ | | | $\frac{1}{8}s^2(\delta_h^0 + \delta_c^0)$ |
| $\gamma_8 = \kappa_8$ | | | $\frac{1}{8}(1-c)^2\delta_h^0 + \frac{1}{8}(1+c)^2\delta_c^0$ |
| $\gamma_9 = \kappa_{10}$ | | | $\frac{1}{32}s^2(\overline{\delta_h^1} + \overline{\delta_c^1})$ |
| $\gamma_{10} = \kappa_9$ | | | $\frac{1}{32}s^2(\delta_h^1 + \delta_c^1)$ |
| $\gamma_{11}$ | $-\frac{1}{16}s(1+c)\overline{\delta_h^1} + \frac{1}{16}s(1-c)\overline{\delta_c^1}$ | $\kappa_{11}$ | $-\frac{1}{16}s(1+c)\delta_h^1 + \frac{1}{16}s(1-c)\delta_c^1$ |
| $\gamma_{12}$ | $-\frac{1}{16}s(1-c)\overline{\delta_h^1} + \frac{1}{16}s(1+c)\overline{\delta_c^1}$ | $\kappa_{12}$ | $-\frac{1}{16}s(1-c)\delta_h^1 + \frac{1}{16}s(1+c)\delta_c^1$ |
| $\gamma_{13} = \kappa_{13}$ | | | $-\frac{1}{16}s(1+c)\delta_h^0 + \frac{1}{16}s(1-c)\delta_c^0$ |
| $\gamma_{14} = \kappa_{14}$ | | | $-\frac{1}{16}s(1-c)\delta_h^0 + \frac{1}{16}s(1+c)\delta_c^0$ |

The relaxation terms are presented as obtained in the $\Pi$ representation (cf. Sec. IV), where the following extra notations are introduced:

$$\hat{\mathbf{\Pi}}^{\mathbf{h}}_{+}=\hat{\mathbf{\Pi}}_{\mathbf{u,g}},\hat{\mathbf{\Pi}}^{\mathbf{h}}_{-}=\hat{\mathbf{\Pi}}_{\mathbf{g,u}},\hat{\mathbf{\Pi}}^{\mathbf{h}}_{\mathbf{z}}=\tfrac{1}{2}(\hat{\mathbf{\Pi}}_{\mathbf{u}}-\hat{\mathbf{\Pi}}_{\mathbf{g}}),$$
$$\hat{\mathbf{\Pi}}^{c}_{+}=\hat{\mathbf{\Pi}}_{l,g},\hat{\mathbf{\Pi}}^{c}_{-}=\hat{\mathbf{\Pi}}_{g,l},\hat{\mathbf{\Pi}}^{c}_{z}=\tfrac{1}{2}(\hat{\mathbf{\Pi}}_{l}-\hat{\mathbf{\Pi}}_{g}). \tag{B2}$$

The relaxation coefficients, $\gamma_1 \ldots \gamma_{14}$ and $\kappa_1 \ldots \kappa_{14}$, are explicitly given in Table VII, in terms of the Fourier transforms of the bath's correlation functions (cf. Table I).

The $\Pi$ representation is equivalent to the dressed-state representation. Hence, Eq. B1 may be compared with the generalized quantum master equation proposed by Kosloff for the parametric amplifier in Ref. 15. The two systems are not identical: one is based on a three-level manifold and the other on two harmonic oscillators. However, an analogy may be drawn between the two if the following correspondence is utilized: $\hat{\mathbf{A}}^{\dagger}\hat{\mathbf{A}}\leftrightarrow\hat{\mathbf{\Pi}}_{u}$, $\hat{\mathbf{B}}^{\dagger}\hat{\mathbf{B}}\leftrightarrow\hat{\mathbf{\Pi}}_{\mathbf{l}}$, $\hat{\mathbf{A}}^{\dagger}\hat{\mathbf{B}}\leftrightarrow\hat{\mathbf{\Pi}}_{+}$, $\hat{\mathbf{A}}\hat{\mathbf{B}}^{\dagger}\leftrightarrow\hat{\mathbf{\Pi}}_{-}$, $\hat{\mathbf{A}}^{\dagger}\leftrightarrow\hat{\mathbf{\Pi}}+h$, $\hat{\mathbf{A}}\leftrightarrow\hat{\mathbf{\Pi}}^{\mathbf{h}}_{-}$, $\hat{\mathbf{B}}^{\dagger}\leftrightarrow\hat{\mathbf{\Pi}}^{\mathbf{c}}_{+}$, $\hat{\mathbf{B}}\leftrightarrow\hat{\mathbf{\Pi}}^{\mathbf{c}}_{-}$. $\hat{\mathbf{A}}=(\hat{\mathbf{a}}+\hat{\mathbf{b}})/\sqrt{2}$ and $\hat{\mathbf{B}}=(\hat{\mathbf{a}}-\hat{\mathbf{b}})/\sqrt{2}$ correspond to the dressed normal modes of the parametric amplifier, where $\hat{\mathbf{a}}$ and $\hat{\mathbf{b}}$ correspond to the annihilation operators of the free oscillators in the rotating frame. Both equations have the semi-group structure[4] in the dressed-state representation, however, the generalized quantum master equation in Ref. 15 is clearly a special case of the more general Eq. B1. To obtain the former from the latter, resonance conditions are assumed (i.e. $\Delta\omega=0$, hence $s=1$, $c=0$) and diagonal coupling terms with the baths are neglected (i.e. $\mathbf{\Delta_h}=\mathbf{\Delta_c}=0$, hence $\gamma_5,\kappa_5 \ldots \gamma_{14},\kappa_{14}=0$). To enhance the comparison, the relaxation coefficients are written as sums of contributions corresponding to the hot and cold baths, such that $\gamma_i=\gamma_i^h+\gamma_i^c$ and $\kappa_i=\kappa_i^h+\kappa_i^c$. Thus the relaxation super-operator may be given by the sum $\mathscr{L}_D(\cdot)=\mathscr{L}_D^h(\cdot)+\mathscr{L}_D^c(\cdot)$ such that

$$\begin{aligned}\mathscr{L}_D^i(\mathbf{X})=&\gamma_1^i([\hat{\mathbf{\Pi}}^{\mathbf{h}}_{+},\mathbf{X}]\hat{\mathbf{\Pi}}^{\mathbf{h}}_{-}+\hat{\mathbf{\Pi}}^{\mathbf{h}}_{+}[\mathbf{X},\hat{\mathbf{\Pi}}^{\mathbf{h}}_{-}])+\kappa_1^i(\hat{\mathbf{\Pi}}^{\mathbf{h}}_{-}[\mathbf{X},\hat{\mathbf{\Pi}}^{\mathbf{h}}_{+}]+[\hat{\mathbf{\Pi}}^{\mathbf{h}}_{-},\mathbf{X}]\hat{\mathbf{\Pi}}^{\mathbf{h}}_{+})+\gamma_4^i([\hat{\mathbf{\Pi}}^{\mathbf{c}}_{+},\mathbf{X}]\hat{\mathbf{\Pi}}^{\mathbf{c}}_{-}+\hat{\mathbf{\Pi}}^{\mathbf{c}}_{+}[\mathbf{X},\hat{\mathbf{\Pi}}^{\mathbf{c}}_{-}])\\&+\kappa_4^i(\hat{\mathbf{\Pi}}^{\mathbf{c}}_{-}[\mathbf{X},\hat{\mathbf{\Pi}}^{\mathbf{c}}_{+}]+[\hat{\mathbf{\Pi}}^{\mathbf{c}}_{-},\mathbf{X}]\hat{\mathbf{\Pi}}^{\mathbf{c}}_{+})+\gamma_2^i([\hat{\mathbf{\Pi}}^{\mathbf{h}}_{+},\mathbf{X}]\hat{\mathbf{\Pi}}^{\mathbf{c}}_{-}+\hat{\mathbf{\Pi}}^{\mathbf{c}}_{+}[\mathbf{X},\hat{\mathbf{\Pi}}^{\mathbf{h}}_{-}])+\gamma_3^i([\hat{\mathbf{\Pi}}^{\mathbf{c}}_{+},\mathbf{X}]\hat{\mathbf{\Pi}}^{\mathbf{h}}_{-}+\hat{\mathbf{\Pi}}^{\mathbf{h}}_{+}[\mathbf{X},\hat{\mathbf{\Pi}}^{\mathbf{c}}_{-}])\\&+\kappa_2^i(\hat{\mathbf{\Pi}}^{\mathbf{c}}_{-}[\mathbf{X},\hat{\mathbf{\Pi}}^{\mathbf{h}}_{+}]+[\hat{\mathbf{\Pi}}^{\mathbf{h}}_{-},\mathbf{X}]\hat{\mathbf{\Pi}}^{\mathbf{c}}_{+})+\kappa_3^i(\hat{\mathbf{\Pi}}^{\mathbf{h}}_{-}[\mathbf{X},\hat{\mathbf{\Pi}}^{\mathbf{c}}_{+}]+[\hat{\mathbf{\Pi}}^{\mathbf{c}}_{-},\mathbf{X}]\hat{\mathbf{\Pi}}^{\mathbf{h}}_{+}),\end{aligned} \tag{B3}$$

where $\gamma_1^h=\lambda_h^+/4$, $\gamma_1^c=\lambda_c^+/4$, $\kappa_1^h=\overline{\lambda_h^+}/4$, $\kappa_1^c=\overline{\lambda_c^+}/4$, $\gamma_2^h=-\lambda_h^-/4$, $\gamma_2^c=\lambda_c^-/4$, $\kappa_2^h=-\lambda_h^-/4$, $\kappa_2^c=\lambda_c^-/4$, $\gamma_3^h=-\lambda_h^+/4$, $\gamma_3^c=\lambda_c^+/4$, $\kappa_3^h=-\lambda_h^+/4$, $\kappa_3^c=\lambda_c^+/4$, $\gamma_4^h=\lambda_h^-/4$, $\gamma_4^c=\lambda_c^-/4$, and $\kappa_4^h=\lambda_h^-/4$, $\kappa_4^c=\lambda_c^-/4$.

In the above formulation, Eq. B3 is very similar to the analogous Eq. 4.1 of Ref. 15. The first two unmixed terms associated with $\gamma_1^i,\kappa_1^i,\gamma_4^i$ and $\kappa_4^i$, are identical in both cases. However, the last two mixed terms are grouped differently in Ref. 15. Namely, $[\hat{\mathbf{\Pi}}^{\mathbf{h}}_{+},\mathbf{X}]\hat{\mathbf{\Pi}}^{\mathbf{c}}_{-}$ is grouped with $\hat{\mathbf{\Pi}}^{\mathbf{h}}_{+}[\mathbf{X},\hat{\mathbf{\Pi}}^{\mathbf{c}}_{-}]$ rather than with $\hat{\mathbf{\Pi}}^{\mathbf{c}}_{+}[\mathbf{X},\hat{\mathbf{\Pi}}^{\mathbf{h}}_{-}]$, as in Eq. B3, etc. The specific pairing in Eq. B3 is important since the two members of each pair are Hermitian conjugates. Thus, if $\mathbf{X}$ is Hermitian, the above pairing would retain this property throughout the evolution, as it should. The different pairing in Eq. 4.1 of Ref. 15 does not share this important property unless $\gamma_2^i=\gamma_3^i$ and $\kappa_2^i=\kappa_3^i$, which is indeed assumed in Ref. 15. However, such an identity is not true in general, as a close examination of the explicit expressions for $\gamma_2^i,\gamma_3^i,\kappa_2^i$ and $\kappa_3^i$ reveals (cf. Table VII).

Thus, the limits of validity of the generalized quantum master equation in Ref. 15 are identified, and its immediate extension is indicated by the present treatment. It is also to be noted that Eq. B1 is far more general since it is applicable outside resonance and may also account for off-diagonal coupling with the bath.


[1] T. Hill, *Statistical Mechanics* (Dover, New York, 1954).
[2] R. Kubo, M. Toda, and N. Hashitsume, *Statistical Physics II—Nonequilibrium Statistical Mechanics* (Springer-Verlag, Berlin, 1983).
[3] H. Spohn and J. Lebowitz, Adv. Chem. Phys. **38**, 109 (1979).
[4] R. Alicki and K. Lendi, *Quantum Dynamical Semigroups and Applications* (Springer-Verlag, Berlin, 1987).
[5] S. Carnot, *Réflections sur la Puissance Motrice du Feu et sur les Machines propres à Dévelopter cette Puissance* (Bachelier, Paris, 1824).
[6] H. Haken, *Laser Theory* (Springer-Verlag, Berlin, 1984).
[7] W. Louisell, *Quantum Statistical Properties of Radiation* (Wiley, New York, 1990).
[8] B. Andresen, R. Berry, M. Ondrechen, and P. Salamon, Acc. Chem. Res. **17**, 266 (1984).
[9] *Finite Time Thermodynamics and Thermoeconomics*, edited by S. Sieniutycz and P. Salamon (Taylor & Francis, New York, 1990).
[10] F. Curzon and B. Ahlborn, Am. J. Phys. **43**, 22 (1975).
[11] P. Salamon and A. Nitzan, J. Chem. Phys. **74**, 3546 (1981).
[12] H. Callen, *Thermodynamics* (Wiley, New York, 1979).
[13] R. Alicki, J. Phys. A **12**, L103 (1979).
[14] R. Kosloff and M. Ratner, J. Chem. Phys. **80**, 2352 (1984).
[15] R. Kosloff, J. Chem. Phys. **80**, 1625 (1984).
[16] E. Geva and R. Kosloff, J. Chem. Phys. **96**, 3054 (1992).
[17] E. Geva and R. Kosloff, J. Chem. Phys. **97**, 4398 (1992).
[18] E. Geva and R. Kosloff, Phys. Rev. E **49**, 3903 (1994).
[19] E. Geva, R. Kosloff, and J. Skinner, J. Chem. Phys. **102**, 8541 (1995).
[20] B. Laird, J. Budimir, and J. Skinner, J. Chem. Phys. **94**, 4391 (1991).
[21] E. Geva, Ph.D. thesis, The Hebrew University, 1995.
[22] A. Abragam, *The Principles of Nuclear Magnetism* (Clarendon, Oxford, 1961).
[23] F. Bloch, Phys. Rev. **102**, 104 (1956).
[24] L. Allen and J. Eberly, *Optical Resonance and Two-Level Atoms* (Dover, New York, 1987).
[25] A. Redfield, Phys. Rev. **98**, 1787 (1955).
[26] C. Slichter, *Principles of Magnetic Resonance* (Springer-Verlag, Berlin, 1990).
[27] F. Bloch, Phys. Rev. **105**, 1206 (1957).
[28] K. Tomita, Prog. Theor. Phys. **19**, 541 (1958).
[29] P. Hubbard, Rev. Mod. Phys. **33**, 249 (1961).
[30] P. Argyres and P. Kelly, Phys. Rev. **134**, A98 (1964).
[31] R. D. Voe and R. Brewer, Phys. Rev. Lett. **50**, 1269 (1983).

[32] A. Yodh, J. Golub, N. Carlson, and T. Mossberg, Phys. Rev. Lett. **53**, 659 (1984).
[33] R. Shakhmuratov and A. Szabo, Phys. Rev. B **48**, 6903 (1993).
[34] E. Hanamura, J. Phys. Soc. Jpn. **52**, 2258 (1983).
[35] E. Hanamura, J. Phys. Soc. Jpn. **52**, 2267 (1983).
[36] E. Hanamura, J. Phys. Soc. Jpn. **52**, 3265 (1983).
[37] E. Hanamura, J. Phys. Soc. Jpn. **52**, 3678 (1983).
[38] M. Yamanoi and J. Eberly, J. Opt. Soc. Am. B **1**, 751 (1984).
[39] A. Schenzle, M. Mitsunaga, R. D. Voe, and R. Brewer, Phys. Rev. A **30**, 325 (1984).
[40] K. Wodkiewicz and J. Eberly, Phys. Rev. A **32**, 992 (1985).
[41] P. Berman and R. Brewer, Phys. Rev. A **32**, 2784 (1985).
[42] S. Y. Kilin and A. Nizovtsev, J. Phys. B **19**, 3457 (1986).
[43] P. Apanasevich, S. Y. Kilin, A. Nizovtsev, and N. Onishchenko, J. Opt. Soc. Am. B **3**, 587 (1986).
[44] M. Yamanoi and J. Eberly, Phys. Rev. A **34**, 1609 (1986).
[45] R. Boscaino and V. L. Bella, Phys. Rev. A **41**, 5171 (1990).
[46] R. Boscaino and F. Geraldi, Phys. Rev. A **45**, 546 (1992).
[47] J. Geusic, E. S. du Bois, R. D. Grasse, and H. Scovil, J. Appl. Phys. **30**, 1113 (1959).
[48] H. Scovil and E. S. du Bois, Phys. Rev. Lett. **2**, 262 (1959).
[49] J. Geusic, E. S. du Bois, and H. Scovil, Phys. Rev. **156**, 343 (1967).
[50] R. Levine and O. Kafri, Chem. Phys. Lett. **27**, 175 (1974).
[51] A. Ben-Shaul and R. Levine, J. Non-Equilib. Thermodyn. **4**, 363 (1979).
[52] W. Lamb, Phys. Rev. A **134**, 1429 (1964).
[53] C. Cohen-Tannoudji, J. Dupont-Roc, and G. Grynberg, *Atom-Photon Interactions, Basic Processes and Applications* (Wiley, New York, 1992).
[54] L. Landau and E. Lifshitz, *Statistical Physics* (Pergamon, London, 1970).
[55] J. Beattie and I. Oppenhei, *Principles of Thermodynamics* (Elsevier Scientific, Amsterdam, Holland, 1979).
[56] D. Evans, R. Coalson, H. Kim, and Y. Dakhnovskii, Phys. Rev. Lett. **75**, 3649 (1995).
[57] A. Aspect *et al.*, Phys. Rev. Lett. **57**, 1688 (1986).
[58] A. Aspect *et al.*, Phys. Rev. Lett. **61**, 826 (1988).
[59] A. Bartana and R. Kosloff, J. Chem. Phys. **99**, 196 (1993).
[60] A. Katsberg *et al.*, Phys. Rev. Lett. **74**, 1542 (1995).